TRANSMITTER LOCATION ESTIMATION USING SOFTWARE DEFINED RADIO

by
Mustafa Tuğrul Özşahin
B.S., Computer Engineering, Yıldız Technical University, 2010

Submitted to the Institute for Graduate Studies in
Science and Engineering in partial fulfillment of
the requirements for the degree of
Master of Science

Graduate Program in Computer Engineering
Boğaziçi University
2014

TRANSMITTER LOCATION ESTIMATION USING SOFTWARE DEFINED RADIO

APPROVED BY:

Assoc. Prof. Tuna Tuğcu (Thesis Supervisor)	....
Assoc. Prof. O. Haluk Bingöl	....
Assist. Prof. Ali Emre Pusane	....

DATE OF APPROVAL: Aug 15, 2014

ACKNOWLEDGEMENTS

I would like to thank everyone who helped and supported me to complete this work and thesis. To those persons I did not mention here by name, I still offer my greatest regards and thanks.

First of all, I would like to thank my thesis supervisor Assoc. Prof. Tuna Tuğcu for many enlightening suggestions and guidance during the development of this thesis, and helpful comments on the thesis text. Without his good will, help, and support, it would not be possible to finish this thesis.

I am grateful to Assoc. Prof. O. Haluk Bingöl and Assist. Prof. Ali Emre Pusane for their participation in my thesis committee and for their helpful comments to improve this thesis.

I would like to offer my deepest thanks to Şükrü Kuran, who has been more than a colleague for me since I started my MSc education, for his mentoring, friendship, kind help, and patience.

I also offer my gratitudes to my colleagues who are also my dear friends Birkan Yılmaz, Salim Eryiğit, and Akif Cem Heren for their friendship, ideas, and support.

Last, I would like to thank my family members for their patience and support through all the phases of my education.

This thesis was supported by the Ministry of Science, Industry and Technology of Turkey under grant number SAN-TEZ 0410.STZ.2013-2 and by Bogazici University Research Fund (BAP) under grant number 7437.

ABSTRACT

TRANSMITTER LOCATION ESTIMATION USING SOFTWARE DEFINED RADIO

This thesis focuses on the practical implementation of transmitter location estimation algorithms using software defined radio devices for the purpose of radio environment map construction, which is used to determine primary user location and available channels for Cognitive Radio. To this end, a testbed is also set up and technical and physical details of this testbed are explained. Using the received signal strength (RSS) data collected from receivers with fixed known locations, the path loss character of an open field line of sight channel is estimated. Then, the location of an immobile transmitter is estimated using the collected RSS data from multiple receivers by applying one proposed and one known technique, and the results of these estimations are explained and compared. The effect of receiver count and the environmental factors on the precision of the results are also explained. To share the gained experimental knowledge, the practical difficulties, tradeoffs, and experiences encountered during the implementation and measurement phases are explained.

ÖZET

YAZILIM TANIMLI RADYO İLE VERİCİ POZİSYONU BELİRLEME

Bu tezde Yazılım Tanımlı Radyo cihazları kullanılarak Bilisel Radyo için birincil kullanıcı yeri ve müsait kanalları tahmin etme açısından önem taşıyan Radyo Ortam Haritası oluşturma amacına yönelik, verici pozisyonu belirleme algoritmalarının pratik uygulaması anlatılmaktadır. Bu amaçla bir deney düzeneği kurulmuş olup, bu düzeneğin teknik ve fiziksel detayları açıklanmaktadır. Ölçülen sinyal gücü kullanılarak sabit konumlu alıcılardan veri toplanmış olup, açık alanda ve görüş hattındaki bir kanalın yol kaybı modeli belirlenmektedir. Ayrıca sabit bir vericinin bilinmeyen pozisyonu, birden fazla yeri bilinen sabit alıcılardan gelen veri ile, önerilen bir metodla ve literatürde bilinen başka bir metodla tahmin edilmekte ve sonuçları karşılaştırılmaktadır. Kullanılan alıcı sayısı ve çevresel faktörlerin, sonuçların isabetliliği üzerindeki etkileri irdelenmektedir. Elde edilen deneysel bilginin paylaşılması amacıyla, uygulama ve ölçümler sırasında karşılaşılan pratik zorluklar, edinilen tecrübeler ve tespit edilen ödünleşimler anlatılmaktadır.

TABLE OF CONTENTS

LIST OF FIGURES

LIST OF TABLES

LIST OF SYMBOLS

d	Distance between the transmitter and the receiver
d_0	Reference distance
H_1	Transmitter height
H_2	Receiver height
PL	Path loss
PL_0	Path loss at the reference distance
P_{rx}	Received power
P_{tx}	Transmitted power
γ	Path loss exponent
$\Gamma(\alpha)$	Reflection coefficient for two-ray model
ϵ_r	Relative dielectric constant of the ground surface
λ	Wavelength

LIST OF ACRONYMS/ABBREVIATIONS

AWGN	Additive White Gaussian Noise
AOA	Angle of Arrival
CF	Center Frequency
CR	Cognitive Radio
CRN	Cognitive Radio Network
dB	Decibel
DFT	Digital Fourier Transform
DSA	Dynamic Spectrum Access
DVB-T	Digital Video Broadcasting - Terrestrial
FCC	Federal Communications Commission
FM	Frequency Modulation
LO	Local Oscillator
LoS	Line of Sight
PCM	Pulse Code Modulation
PU	Primary User
RF	Radio Frequency
RSS	Received Signal Strength
SDR	Software Defined Radio
SU	Secondary User
TOA	Time of Arrival
UHF	Ultra High Frequency
VHF	Very High Frequency

1. INTRODUCTION

Current state of the frequency spectrum for wireless communications is based on the fixed allocation of the frequency bands to known registered parties/technologies. This fixed allocation and current regulations on the usage of the spectrum limits the adaptation of new wireless communication systems to fast growing bandwidth demands of present wireless applications. Consequently, some frequency bands are under-utilized, while some are densely used. This type of unbalanced spectrum usage causes spectrum scarcity. To alleviate this problem, the Cognitive radio (CR) concept has been proposed in the telecommunication literature. CR is a radio that can change its transmitter parameters based on the interaction with the environment in which it operates.

The CR term was first mentioned by J. Mitola III in 1999 [4]. According to Mitola, Software Defined Radio (SDR) provides an ideal platform for the realization of CR. SDR is a set of technologies for defining radio transceiver parameters and functions in software, including carrier frequency, modulation bandwidth, channel coding, and frequency/space/time/code agility. SDR started to come out in early 90's, with the thinking of programming the hardware of traditional analog radio technology by software.

In [5], Simon Haykin defines the CR as an intelligent wireless communication system that is aware of its surrounding environment. In his definition, the CR has two primary objectives:

- highly reliable communications whenever and wherever needed,
- efficient utilization of the radio spectrum.

The CR concept is built on the idea of dynamic spectrum access (DSA). In this concept, the parties who are allocated the privileged use of a channel are called the primary users (PU). While a channel is not being used by PU in a certain slice of time in a given geographical area, and if this unused slot can be known or detected correctly, the channel could be utilized by the secondary users (SU), who are the less privileged opportunistic users. PUs have the license to operate in a spectrum band. Therefore they are also called the licensed users. SUs have no spectrum license and they need additional cognitive functionalities to share the licensed spectrum band. For this reason, they are also called the unlicensed users or CR users. One important aspect of sharing frequency bands between PUs and SUs is the SUs must not harm the communication of a PU.

CR system consists of four main functions: spectrum sensing, spectrum sharing, spectrum decision, and spectrum mobility. Among these functions, spectrum sensing is the one we focus in this thesis. It is the work of determining which portions of the spectrum is available and detecting the presence of licensed (primary) users when a user operates in a licensed band.

Spectrum sensing is mainly done by the measurement capable devices (MCD) in the network. Sensing might be non-cooperative where CR users detect the primary transmitter signal independently through their local observations, or it might be cooperative where information from multiple CR users are utilized for primary user detection.

Detection methods in CR can be put into three main classes: Transmitter detection, receiver detection and interference temperature management. Since we study transmitter location estimation in this thesis, transmitter detection is the one we focus. There are three categories of transmitter detection methods in the literature: matched filter detection, energy detection and cyclostationary feature detection [6]. In cyclostationary detection, the periodical features of the modulated signals like sine wave carriers, cyclic prefixes, or pulse trains are detected by analyzing their spectral correlation. Matched filter detection is used when the shape of the PU's signal is known, by matching the receiver's filter to the shape of the signal to obtain the optimal detector. When there is not sufficient information about the shape or the periodicity of the signal, energy detection method can be used to sense the presence of a PU signal.

The energy of the signal is obtained by squaring the output signal of the receiver's band pass filter. We use this approach in this thesis to determine the presence of the transmitter and the received power at the receiver antenna.

Sensing and detection is not always sufficient for establishing a complete environmental awareness for a Cognitive Radio Network (CRN). For that reason, the Radio Environment Map (REM) concept is proposed. Essential functionality of a REM is the construction of dynamic interference map for each frequency at each location of interest. REM collects spectrum measurements from the nodes with spectrum sensing capabilities. These nodes might be the CRs in the network or dedicated spectrum sensors, which are referred to as MCDs [7]. It generates a spectrum usage map by processing these data. REM construction methods in the literature can be put into two main classes: spatial statistics based methods and transmitter location estimation based methods.

In this thesis, we study practical implementation of transmitter location estimation for REM construction purpose. We set up a testbed, and taking sufficient amount of measurements, first we estimate the channel path loss properties for the open field. Then, we investigate the possibilities of estimating the unknown location of transmitter using the sensing data coming from multiple receivers. We propose a method to estimate transmitter location, apply it to the sensing data, and show the results of the estimation. We also test and validate the usability of a known transmitter location estimation based REM construction method given in [2] by practical implementation.

1.1. Contributions of this Thesis

The contribution of this thesis can be summarized as follows:

- This thesis evaluates and gives information about the practical applicability of a transmitter location estimation method: LIvE REM Construction [2].
- Using a testbed, it explains the procedures to estimate and decide an appropriate path loss model for an open field LoS channel. It compares the fitness of the

models to the application environment.

- It exploits the practical issues and technical difficulties of setting up a testbed on an open field for transmitter location estimation using SDR devices.

1.2. Thesis Outline

The outline of this thesis is as follows: First, in Chapter 2 we review the literature and summarize the work done on CR, spectrum sensing, REM, and transmitter location estimation.

In Chapter 3, the testbed we assemble to estimate channel specifications of the open field and taking measurements for applying our transmitter localization methods is explained.

The experiments done for path loss and transmitter location estimation and their results are explained in Chapter 4. In this chapter the procedure followed to estimate the channel path loss characteristics and transmitter location are detailed. A method is proposed to estimate the transmitter location and it is applied to the data collected from the experiments. Another known method is also applied and its performance is validated.

Finally, Chapter 5 concludes the thesis by explaining the practical difficulties and experiences encountered while applying the ideas to a real world environment, summarizing the work and elaborating a discussion on the possible future applications.

2. RELATED WORK

2.1. Cognitive Radio

Current wireless networks operate on the statically allocated spectrum. Most of the spectrum is allocated to various institutions by the spectrum management agencies according to long-term agreements. These allocations are generally long-term agreements between the licensed users and the authorities. Thus, a licensed band is forbidden to any other user than the license holder, whether used or not. As a result of this situation, a large portion of the spectrum remains underutilized [8]. Since the demand for higher data rates and bandwidth increases, the spectrum with the fixed allocation scheme becomes insufficient for the requirements of the developing wireless applications.

This inefficiency in the spectrum usage brings the need for a new communication paradigm. CR concept is proposed to exploit new opportunities and bring on better allocation mechanisms to spectrum access [4]. Federal Communications Commission (FCC) formally defines CR as a radio that can change its transmission parameters based on the interaction with its environment. It is based on the DSA concept, which allows cognitive wireless devices to use the licensed bands opportunistically while it is not being used by the PUs who hold the license for the band.

Since the CR devices need to dynamically change their transmission parameters and adapt to the environment, SDR is cut out for the realization of this idea. A transceiver is referred to as a SDR if its communication functions are implemented as running programs on an appropriate processor. Transmitter and receiver algorithms are implemented and configured in software based on the same hardware. A CR is an SDR which senses the communication environment, tracks the changes, and reconfigures its communication scheme according to these changes [9].

CR has different functions to accomplish the task of opportunistic spectrum usage

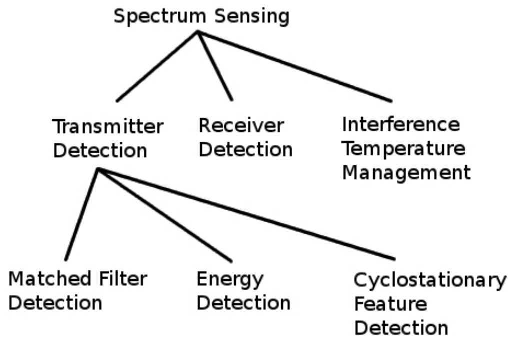

Figure 2.1. Classification of the spectrum sensing techniques.

and efficient utilization. These functions can be put into four categories and summarized as follows:

- *Spectrum sensing* is the function of determining the presence of the PUs and the occupied channels, and which channels are available for usage of the SUs.
- *Spectrum decision* is the determination of the best available channel.
- *Spectrum sharing* is the work of coordinating access to the available channels.
- *Spectrum mobility* is the function of vacating the channel in case of a PU's arrival, and handing off the channels.

2.2. Spectrum Sensing

Since we focus on the transmitter location estimation for REM construction purpose in this work, we explain spectrum sensing in more detail. The most important function of the CR is spectrum sensing because the origin of the problem is the sparse use of the spectrum and the purpose is to exploit the unused portions (spectrum holes) and make better use of them.

There are three main detection approaches for spectrum sensing: transmitter detection, receiver detection and interference temperature based detection. Figure 2.1 visualizes this classification.

Receiver detection is based on the detection of the local oscillator (LO) leakage power the PU receivers emit when they receive the signals from the transmitter. However, the LO leakage signal is typically weak, thus, the implementation of a reliable detector is not trivial. Currently this method is feasible for only the detection of the TV receivers [10].

Interference temperature is an approach for limiting the SU's transmission power at such a level that the accumulated received power should be no more than a prescribed noise floor at a certain distance from the transmitter. However, constraining the transmitter power at a certain level is not trivial because of the highly mobile usage and variability of radio frequency (RF) emitters, since new sources of interference may appear [11]. The interference temperature model has been introduced by the FCC for measuring the interference at the receiver [12]. Through the interference temperature limit, the model manages interference at the receiver, which is the amount of new interference the receiver could tolerate. As long as the SUs don't exceed this level, they can use the band [8]. Although the interference temperature model is dropped by the FCC, it is still being studied for quantification of the interference level at the PU receivers [13].

Transmitter detection is the most common approach in spectrum sensing and it is based on detecting the received signal at the SUs coming from the PUs. Transmitter detection is basically a decision between two hypotheses [14]:

$$\begin{aligned} x(t) = &\quad n(t) \qquad H_0, \\ x(t) = &\quad hs(t) + n(t) \quad H_1 \end{aligned}$$

where $x(t)$ is the signal received by SU, $s(t)$ is the transmitted signal, h is the complex gain of the channel, and $n(t)$ is the Additive White Gaussian Noise (AWGN). H_0 is the null hypothesis stating that there is no transmission detected from a PU, and H_1 states that a PU's transmission is detected.

For transmitter detection, there are three main approaches in spectrum sensing: matched filter detection, cyclostationary feature detection, and energy detection.

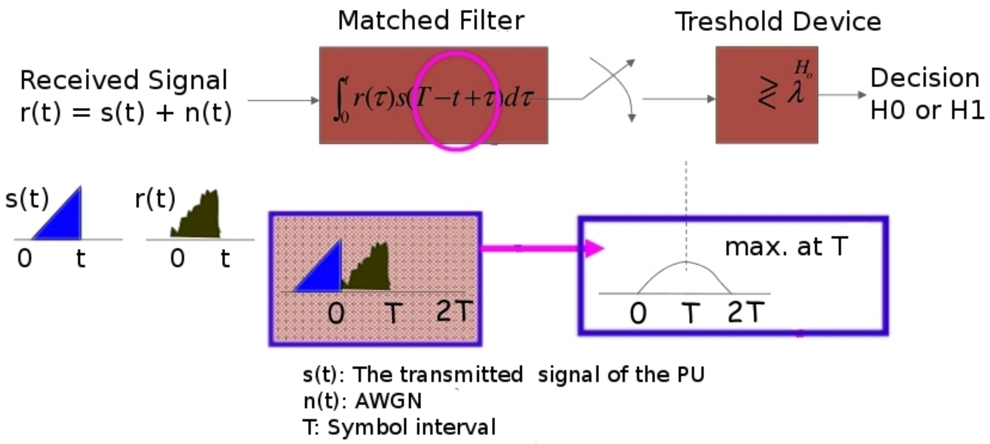

Figure 2.2. Illustration of the Matched Filter approach.

2.2.1. Matched Filter Detection

If the SUs have information about the PU signal's properties like the operating frequency, modulation, and bandwidth, they can match the receiving filter according to these properties and design an optimum receiver. This method provides a high probability of detection and decreases the risk of missed detection or false alarm [11], but the implementation cost and the power consumption is high compared to the other methods [6]. However, if this information is not accurate, matched filter method performs poorly. Figure 2.2 illustrates the match filter detection approach.

2.2.2. Cyclostationary Feature Detection

Cyclostationary feature detection is the approach of detecting the features in the transmitted PU signals like sine wave carriers, pulse trains, repeating spreading, hopping sequences, or cyclic prefixes, which result in built-in periodicity. It was first introduced in [15]. Cyclostationary feature detectors are utilized to differentiate the PU signals from the noise, by analyzing a spectral correlation function.

2.2.3. Energy Detection

Energy detection, also known as the radiometry or periodogram, is the most applicable and the most commonly used transmitter detection method for spectrum sensing. It is more appropriate for high signal-to-noise (SNR) ratios. For the cases where the receiver cannot gather specific information about the PU's signal other than its operating frequency, an energy detector is the optimal detector [16]. It only measures the received signal strength (RSS) value at a certain frequency band, rather than any periodic feature of the signal.

To measure the energy of an incoming signal at a certain band, receiving side applies a band pass filter to the signal to get the components in only the requested band. Then, the output of the filter is squared and integrated [17]. We use this approach in this work to get measured RSS values from our RTL-SDR receivers which is explained in Section 3.2.2.1.

Figure 2.3 shows the block diagrams of the receivers for these three mentioned detection methods: matched filter detector (a), energy detector (b), and cyclostationary feature detector (c). These blocks in the diagram might be applied as hardware components, or as digital signal processing software components for SDR.

2.2.4. Cooperative Sensing

Sensing can be classified as cooperative and non-cooperative, according to the information usage and synthesis scheme used to decide on a PU transmitter's presence. If one SU decides based on its own local measurements, it is considered as non-cooperative sensing. If the sensing information from multiple SU receivers are considered to make a decision, it is considered as cooperative sensing.

Cooperation of SUs for successful sensing limits the number of channels that can be sensed. As a result, the utilization is affected by the number of sensing nodes. Thus, a subset of the channels can be selected considering the traffic requirements, and the

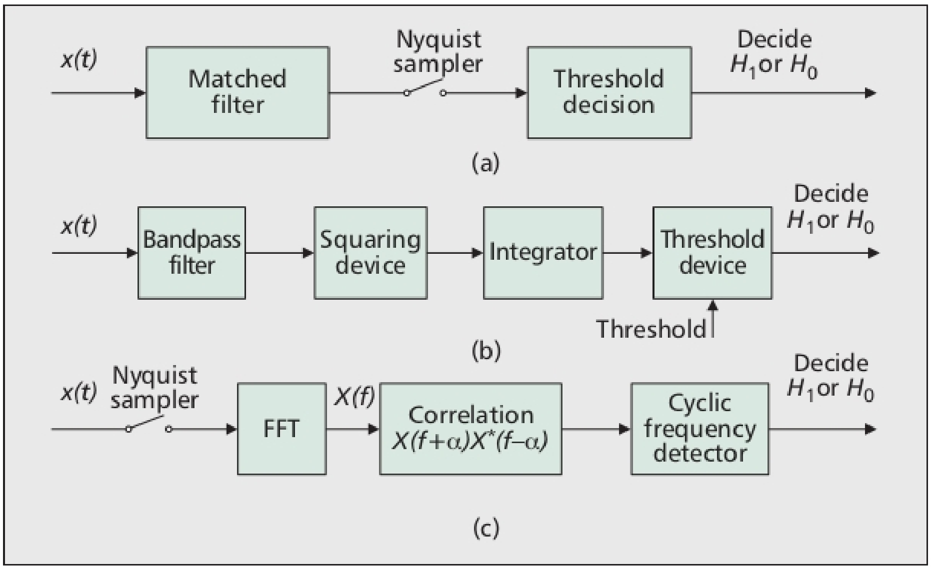

Figure 2.3. Block diagrams for transmitter detection methods [1].

SUs can be assigned to those channels for sensing. In [18], the problem of channel and user selection is considered for cooperative sensing.

Detection with cooperation among multiple SUs is more accurate compared to non-cooperative sensing. However, cooperation also increases the energy consumption of the network. Since the devices in a CRN are generally mobile devices with local power sources, optimizing the tradeoff between the accuracy and the energy consumption is also important for feasibility of the system [19].

2.3. Radio Environment Map

Instant information of detected PU signals gathered from the individual CR devices is not always sufficient for establishing a systematic way of decision of available spectrum bands. The occupancy of some licensed bands may vary from time to time, and this usage scheme can even be periodic, or usage intervals of some licensed bands may be completely unpredictable. Moreover, some bands might be heavily used in some regions, and not used at all in another region. For such reasons, establishing a more systematic knowledge base for spectrum occupancy information is essential [20].

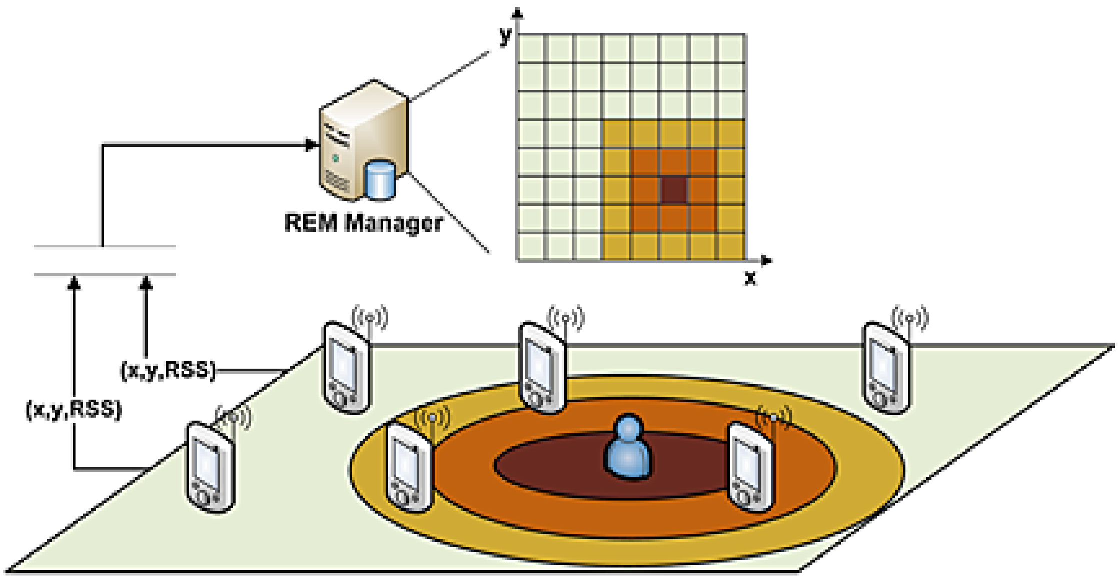

Figure 2.4. A REM system model [2].

REM, first defined as an abstraction of the real-world environment, which stores multi-domain information such as PUs, policies, or terrain data [21]. However, it can be also generalized as a cognitive network entity that can derive new information from the gathered data, interpret the spatio-temporal properties, and come up with a map of the RF environment [22]. Utilizing the REM as an intelligent decision mechanism and information source is a promising idea because it reduces the processing and information sharing burden on the cognitive devices and offers more environmental awareness than the individual devices can acquire. Figure 2.4 shows an illustration of a REM operating over an area.

The data REM stores can be classified as: static, volatile, and derived data[7]. The static data represents the entities which are not changeable over time, like the location of the CR base stations, or operators in a region. The volatile information, on the other hand, is the information about the entities in the environment which are highly dynamic like the locations and the activities of the CR users. REM keeps its information up to date dynamically by tracking the changes in the environment. The derived data in REM is the data which the REM infers by tracking these changes and making deductions about the RF environment.

REM construction techniques in the literature are examined under two main categories: spatial statistics based techniques [23], and transmitter location estimation based techniques [24]. These two approaches can also be named as direct and indirect approaches, respectively.

Making use of the spatial correlational structure of a given area, spatial statistics describe the statistical properties of the area in which the REM is operates on by fusing the data from the area of concern. The fusion of the data is based on different interpolation techniques like Kriging, inverse distance weighted, and nearest neighbor interpolation. A spatial statistic based REM construction approach using massive amount of measurements from the environment is studied in [25].

If the locations of the active transmitters are known or can be estimated, this information would ease the REM construction. Transmitter location estimation based REM construction methods tend to make use of this information by estimating the locations of the transmitters using the RSS data from CR devices or dedicated receivers in the network. [26] studies REM construction by estimating the transmitter locations using the RSS information from heterogenous receivers in the network.

2.4. Transmitter Location Estimation

Estimating the location of a transmitter is an issue of interest for many kind of applications. Different received signal parameters like Time of Arrival (TOA), Angle of Arrival (AOA), and RSS can be utilized for this purpose [27].

Since path loss models estimate the amount of decrease in the RSS value through distance, RSS at the receiver gives an idea about the distance of the transmitter when it is interpreted using a path-loss model. Figure 2.5 illustrates the estimation of a transmitter's distance using the RSS value using a path loss model with a gaussian error variable.

The angle of a transmitter can be estimated using the AOA of a signal at the

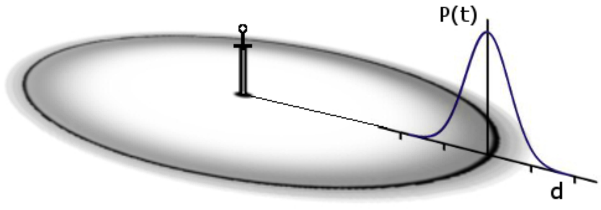

Figure 2.5. Estimating distance of a transmitter using a path loss model with a Gaussian error.

receiver. AOA of a signal is generally estimated using antenna arrays [28]. If the antenna array's geometry is known, difference between arrival times of a signal in the elements of antenna array gives the angle information about the signal.

Estimating the flight time of a signal, TOA parameter may also give information about the distance of the transmitter from the receiver. However, this information may not always be available because it requires a synchronization mechanism between the transmitter and the receiver, like a mutual clock or a time exchange protocol. TOA of a signal is generally detected using matched filters, or cyclostationary feature detectors. In [29], a TOA based localization technique is applied by minimizing the internal delay errors of the receivers.

Using these parameters (RSS, TOA, AOA), a transmitter can be localized by making use of geometric methods. Using distance information from at least three sensors, the location of the transmitter can be estimated using the trilateration method as shown in Figure 2.6. Also, using the AOA information from at least two sensors, the location of the transmitter can be estimated using triangulation method [30]. These parameters and methods can also be used together for a hybrid estimation.

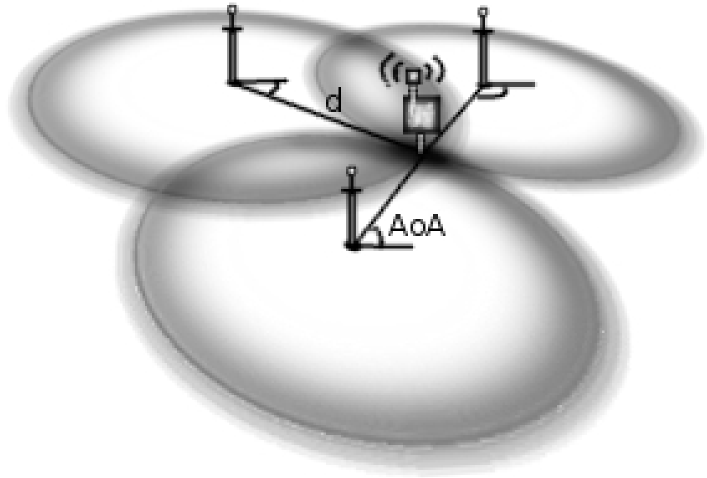

Figure 2.6. Fusion of the estimations from different sensors.

2.5. Path Loss Models

Path loss is the difference (in dB) between the transmitted power and the received power. It represents signal level attenuation caused by free space propagation, reflection, diffraction and scattering. Path loss is an important component to determine the link budget of a communication system. Path loss models in the literature are examined under two main classes: empirical (or statistical) models and deterministic models.

2.5.1. Deterministic Models

Deterministic models are based on the physical laws of wave propagation. These methods require complete knowledge about the environmental objects as obstacles or reflection sources like buildings, roads, roofs, doors or walls. They tend to produce more accurate results than empirical models. However, they have more parameters and they require more computational power.

2.5.1.1. Ray Tracing. In theory, electromagnetic wave propagation characteristics of a channel could be computed with complete environmental geometry knowledge. Since

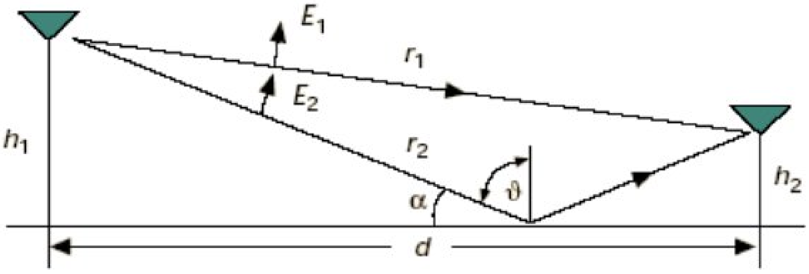

Figure 2.7. Two-ray model [3].

the high frequency radio waves have a ray-like behavior, by using the concept of ray-tracing, waves coming from different multipath sources and their effects on received signal power can be calculated using physical equations [3].

2.5.1.2. Two-Ray Model. Two-ray (ground reflection) Model is a radio propagation model that predicts path loss for the cases when there is a LoS channel between the transmitter and the receiver, and there is a flat ground as a predominant reflection source. Since the measurements are done on a flat field with LoS channel, this model fits to the case of our testbed. Figure 2.7 shows a typical case of a two-ray channel. Figure 2.8 shows a typical behavior of the RSS value calculated by the two-ray path loss model in logarithmic scale.

Due to their phase difference at the receiver, the two waves can have a constructive or destructive effect on the received signal power. The LoS distance from transmitter to the receiver affects the phase and magnitude of the direct wave. The magnitude and phase of the reflected wave is affected by the reflection coefficient Γ and the total traveled distance, which is the sum of the distance from transmitter to the reflection point, and the distance from reflection point to the receiver [31].

Assuming the distance between the transmitter antenna and the receiver antenna is d, transmitter antenna height is h_1, and receiver antenna height is h_2, the received signal power P_r is calculated by summing the contributions of each ray. The received

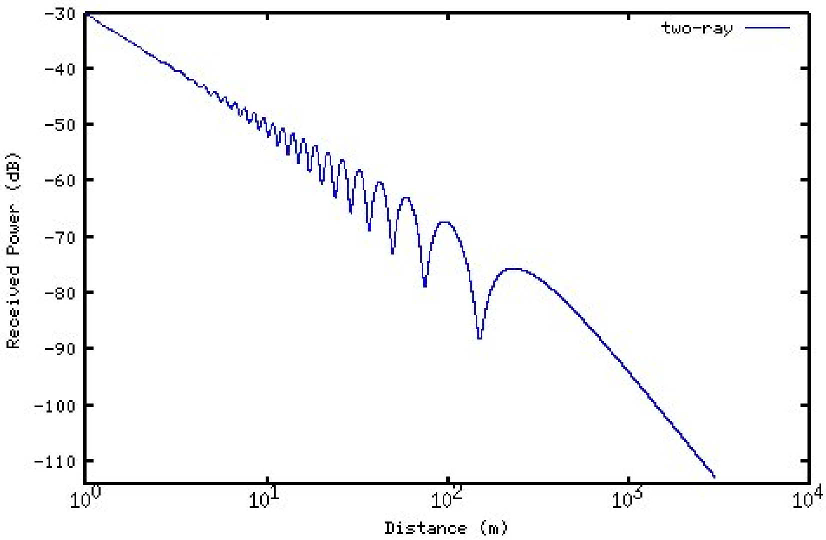

Figure 2.8. Typical behavior of the two-ray path loss model curve in logarithmic scale.

power is calculated as:

$$P_r = P_t(\frac{\lambda}{4\pi})\left(\frac{1}{r_1}e^{(-j2\pi r_1)} + \Gamma(\alpha)\frac{1}{r_2}e^{(-j2\pi r_2)}\right)^2$$

where P_t is the transmitted power, r_1 is the distance of the direct wave which can be calculated using geometry, r_2 is the distance from the transmitter to the reflection point, and $\Gamma(\alpha)$ is the reflection coefficient. $\Gamma(\alpha)$ depends on the angle of reflection (α) and the polarization of the electromagnetic wave.

The reflection coefficient is calculated as:

$$\Gamma(\alpha) = \frac{\cos\Theta - a\sqrt{\epsilon_r - \sin^2\Theta}}{\cos\Theta + a\sqrt{\epsilon_r - \sin^2\Theta}}$$

where $\Theta = 90 - \alpha$ and $a = 1/\epsilon$ for vertical polarization or 1 for horizontal polarization. ϵ_r is a relative dielectric constant (also called the relative permittivity) of the ground surface [3]. Since we know the distance d of each measurement and the transmitter and the receiver heights, h_1 and h_2, we tune this parameter to fit our data to the two-ray model and to come up with the estimated relative permittivity constant of our ground surface.

2.5.2. Empirical Models

The empirical models are the path loss models based on observations and measurements [32]. These models have few parameters and they use statistical data. They are generally less accurate than deterministic models, but they reduce the complexity of the calculations and the estimations.

2.5.2.1. Log Distance Model. Theoretical models and results of measurements done for path loss show that the average RSS decreases logarithmically with distance in radio channels [33]. The most general empirical path loss model is the log-distance model. In this model, the path loss increases logarithmically in dB. The path loss formula of this model is:

$$PL = P_{tx} - P_{rx} = PL_0 + 10\gamma \log_{10}(d/d_0)$$

Where PL is the path loss (in dB), P_{tx} is transmitted power, P_{rx} is received power, d is the distance between the transmitter and the receiver, d_0 is the reference distance. (1 meter in our calculations), PL_0 is the path loss at the reference distance (in dB), and γ is the path loss exponent.

Path loss exponent γ is different for each type of channel. It is 2.0 for free space. For different type of channels (i.e. indoor, outdoor, urban, etc) γ is found empirically by measurement statistics. We tune this parameter to fit our measured path loss-distance data to the model.

In this work, we apply the two-ray and the log-distance models to our path loss data. To give an intuition about their behavior, Figure 2.9 shows a curve of log-distance model with $\gamma = 2$, which is the path loss exponent of the free space, and two ray model with ground reflectivity coefficient $\epsilon_r = 2$ with H_1 and H_2= 1.35.

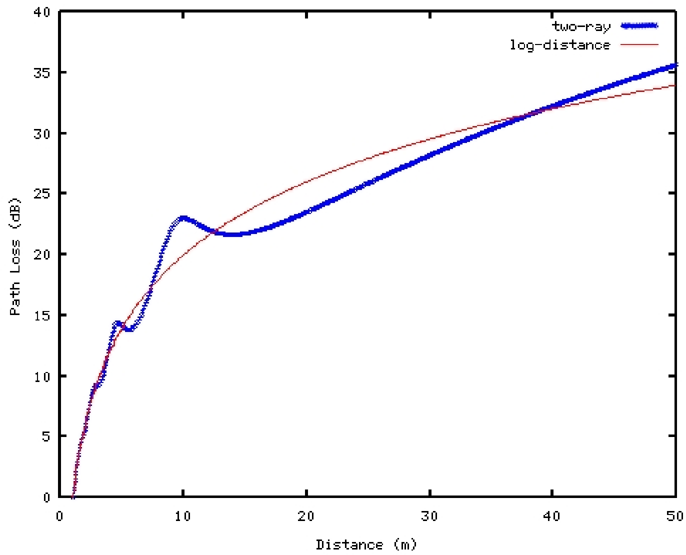

Figure 2.9. Comparison of the behaviors of log-distance and two-ray models for path loss at a 50m range.

2.5.2.2. Standard Empirical Models. There have been measurement campaigns in the literature to define reliable empirical models for wireless network design, such as Okumura-Hata, COST-231 Hata model, Walfisch-Ikegami, etc. These methods are also known as radio wave propagation models and are generally used for designing mobile wireless networks.

One of the most commonly used empirical model for the systems operating in very high frequency (VHF) or ultra high frequency (UHF) bands is Okumura-Hata model, which is developed from the extensive measurements of Y. Okumura and M. Hata. It is based on the measurements taken in certain urban, sub-urban and rural areas of Japan. It is recognized by the International Telecommunications Union (ITU) under the ITU-R Recommendation P.529 [34].

Another famous standard path loss model for mobile wireless systems is the COST-231 Hata model which is an extension to the Hata-Okumura model. It is designed for the frequency band from 500 MHz to 2000 MHz and includes corrections for urban, suburban and rural environments which makes it a widely used model [32].

3. THE TESTBED

In this section, the physical environment and the devices used in the experiments are explained. The methods followed during the experiments are also detailed.

3.1. The Environment

For the measurements in this work, an empty field in the Kandilli campus of the Boğaziçi University is used. The ground is nearly flat and there are no obstacles inside the field, but there are considerable amount of trees and other buildings surrounding the field. Since all the measurements are taken for LoS cases, the effect of the buildings outside the area and the trees are ignored. Their multi-path effects on the measurements are considered as noise.

3.2. Devices and Software

3.2.1. Transmitter

The transmitter used in this work is a wireless microphone transmitter with model Sennheiser-ew100g3, which is shown in Figure 3.1(A). It is a mobile transmitter which works with a pair of AA batteries. It transmits Pulse Code Modulation (PCM) sound data using Frequency Modulation (FM) between 780 and 822 MHz. We used 782.1 MHz channel for all the measurements in this work. It converts the sound from its analog microphone to PCM data, then transmits it using FM. PCM is a method to digitally represent sampled analog signals. We unplug the microphone from the audio input jack so that it always transmits the data of a completely quiet voice. Since the data transmitted is always the same, the power of the transmission does not fluctuate over time.

The typical RF output power of this device is 30 mW, but the measurements showed that the transmission power can decrease over time due to the battery condi-

Figure 3.1. The transmitter powered with an external adapter on a tripod.

tion. To avoid this unstable condition during the experiments, we have powered the transmitter with an external power adapter. This provides the transmitter the ability to transmit with the same power for a long duration. Figure 3.1(B) shows the transmitter on its portable tripod and powered with an external power adapter.

3.2.2. Receivers

The most important devices in this work are the receivers. The main purpose of a receiver is to measure the RSS in a certain frequency band at its physical location. The requested band is set by the software and is re-configurable.

The device used as a receiver in this project is a Digital Video Broadcasting - Terrestrial (DVB-T) receiver dongle based on RTL2832U chipset. The device itself is shown in Figure 3.2 and it is primarily built for digital TV and FM radio reception. But thanks to its UNIX driver and library librtlsdr, the raw data can be read as 8 bit I/Q samples with software. I/Q is a data type used to represent the changes in magnitude and phase of a sine wave. This feature enables us to convert this device to a wideband SDR receiver. Throughout the rest of this thesis, we refer to this device as RTL-SDR.

Figure 3.2. DVB-T receiver dongle and its antenna.

The frequency range of the receiver is determined by its tuner. Different RTL-SDR dongles may have different tuners inside. In this work, a dongle with Rafael Micro R820T tuner is used, and its frequency range is from 24 MHz to 1766 MHz.

The RTL-SDR has a theoretical maximum sampling rate of 3.2 MS/s (megasamples per second). However, according to the host machine USB speed, some samples might be dropped at this rate. 2.048 MS/s is the optimum sample rate without the risk of dropping samples. Thus, for the measurements we read the data with a rate of 2.048 MS/s for reliability.

The dongle has an analog-digital converter with 8 bit resolution. It streams the raw signal data as complex samples, 1 byte I and 1 byte Q interleaved. Each received data has a size of 1 byte, which is is between 0 and 255. We normalize it by converting it to a float value between -1.0 and +1.0 in the software before making power calculations.

3.2.2.1. Measuring the Received Signal Strength of a Transmission. The Linux C/C++ library of RTL-SDR has suitable functions to set the sample rate, tuner gain, and the center frequency of the receiver. This allows us to tune into any channel by software control. After setting the parameters and center frequency, we can call the proper functions of the library to read an arbitrary amount of samples synchronously or asynchronously.

We perform all the receiver-related configurations, data reading, processing, and

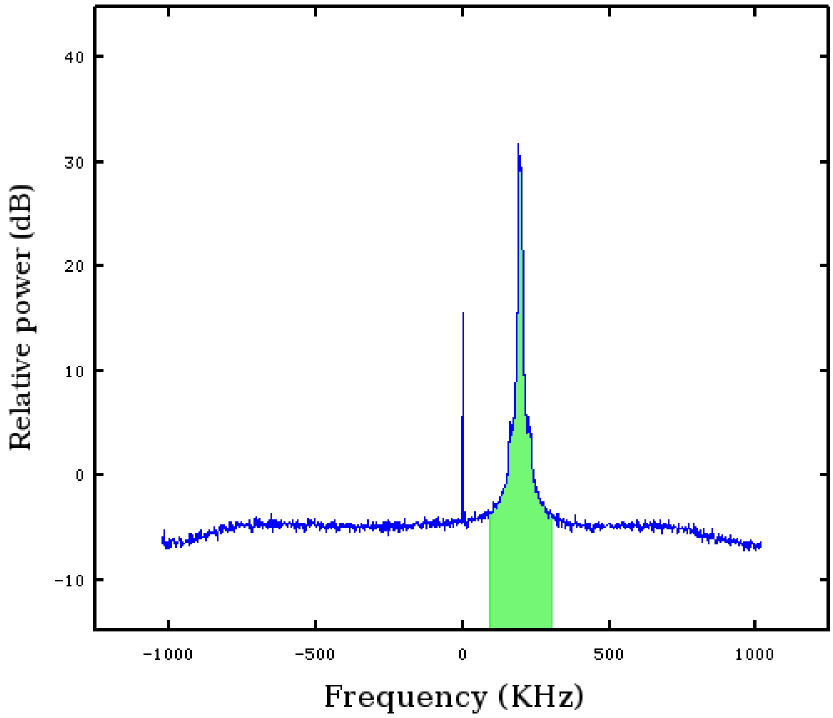

Figure 3.3. A frequency-power plot of the spectrum in a 2 MHz band.

power calculations in a single C++ program. The program repeatedly reads an amount of raw data from the device (for 0.125 seconds), and calculates its frequency domain amplitudes by applying Digital Fourier Transform (DFT) to the data. We use Linux built-in fftw library to perform the DFT operation on the raw data.

By applying DFT on the raw samples read from the RTL-SDR, we obtain received power at each frequency bin in decibels (dB). Figure 3.3 shows a plot of the frequency domain data of a portion of read samples at center frequency: 781.9 MHz. In the plot there is a transmission visible at 782.1 MHz frequency, which is the transmission from our transmitter, the wireless microphone.

To calculate the power of a transmission in dB, we simply concatenate the powers of all the bins in its band. Although the specifications of the transmitter imply that it uses 50 KHz bandwidth, we consider 200 KHz of bandwidth around its frequency because our measurements on the power spectrum indicates that its effective bandwidth is 200 KHz. Figure 3.3 shows this affected spectrum band and the green slice in this

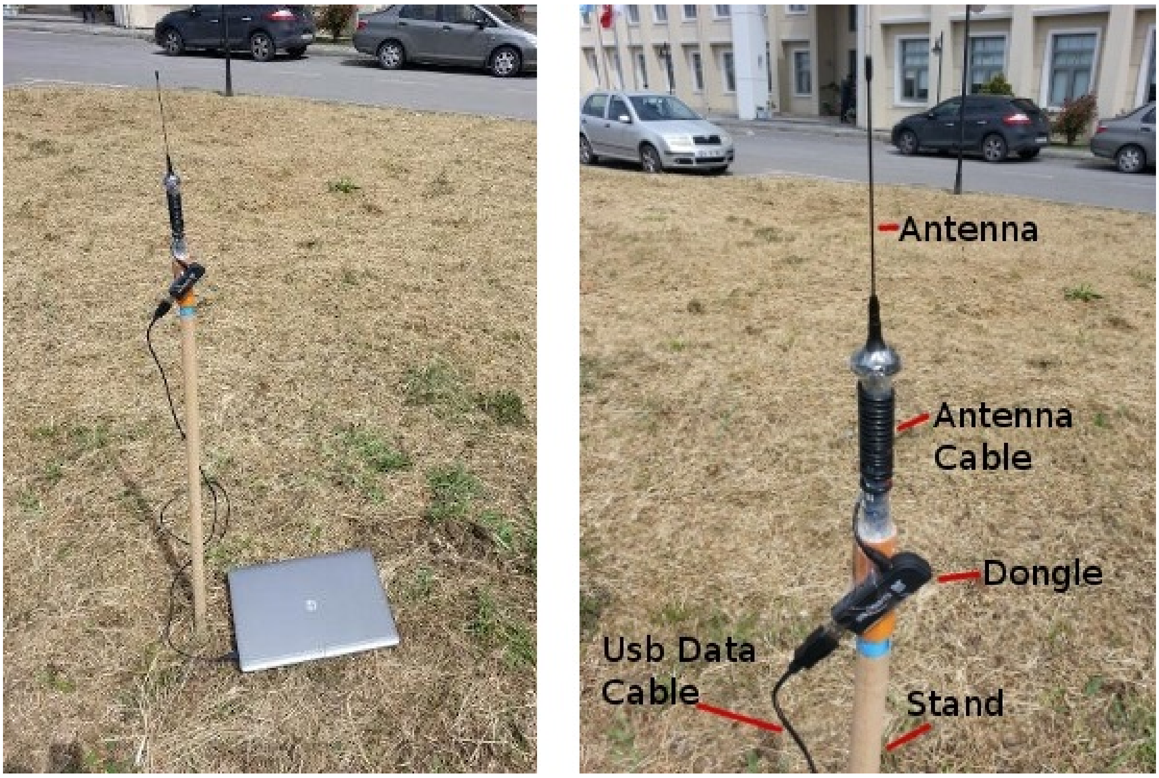

Figure 3.4. RLT-SDR receiver and its antenna placed on top of a stand.

figure indicates the part of the frequency spectrum which is used to come up with the total power of the transmission.

3.2.2.2. Receiver Placement and Antenna Configuration. When a measurement is meant to be performed from a certain position, the receiver device is placed onto the corresponding stand. The receiver assembly consists of the RTL-SDR dongle, its antenna and the antenna cable, a laptop and a USB extension cable to carry the data to the computer. Figure 3.4(A) shows a receiver placed on one of the stands.

The receiver's antenna and its antenna cable are both able to receive signals. Experiments showed that when the dongle is connected directly to the computer and the antenna is placed at top of the stand, the position and shape of the antenna cable has a great effect on the received signal's power. For that reason, we had to gather all the receiving parts of the receiver assembly together and place them at the top of the stand so that all the receiving parts are on the line-of-sight (LoS) of the transmitter. Figure 3.4(B) shows a detailed view of this antenna configuration.

4. MEASUREMENTS AND TRANSMITTER LOCATION ESTIMATION

This section explains the experiments and measurements done using the system and devices explained in Chapter 3, and discusses the results of these experiments.

4.1. Examining the Path Loss Model of the Environment

To determine the most appropriate path loss model for the environment, a series of measurements have been performed. Appropriate path loss models for our LoS case are examined and fitted to the measurement data using the least squares method.

The transmitter is placed on a stable stand which is 1 meter high, and the receiver assembly is put on a mobile tripod which is also 1 meter high. Starting from the nearest position to the transmitter, a series of measurements is taken at each meter from 1 to 50 meters. As a result of this work, we had a series of data written to the receiver's disk by the power-calculating receiver program mentioned in 3.2.2. This 50m measurements are performed for three different routes, which are shown in Figure 4.1

This measurement operation gives a collected power data like the one shown in Figure 4.2, which is only a part (2-5m) of the whole measurements (1-50m) for a detailed illustration. When there is no mobile objects near the transmitter and the receiver, the RSS values does not fluctuate very much. The flat parts of the plotting indicates a stable measurement duration when the receiver is placed at a known distance and there are no moving objects around like a person. The fluctuating parts indicates the time when the experimenter comes near the receiver and repositions it. Since a person near the transmitter or the receiver affects the RSS value significantly, only the RSS values taken when the experimenter is far from the field are considered. Mean of the values in each stable environment duration is considered as the RSS value of the corresponding distance.

Figure 4.1. Routes for path loss measurements.

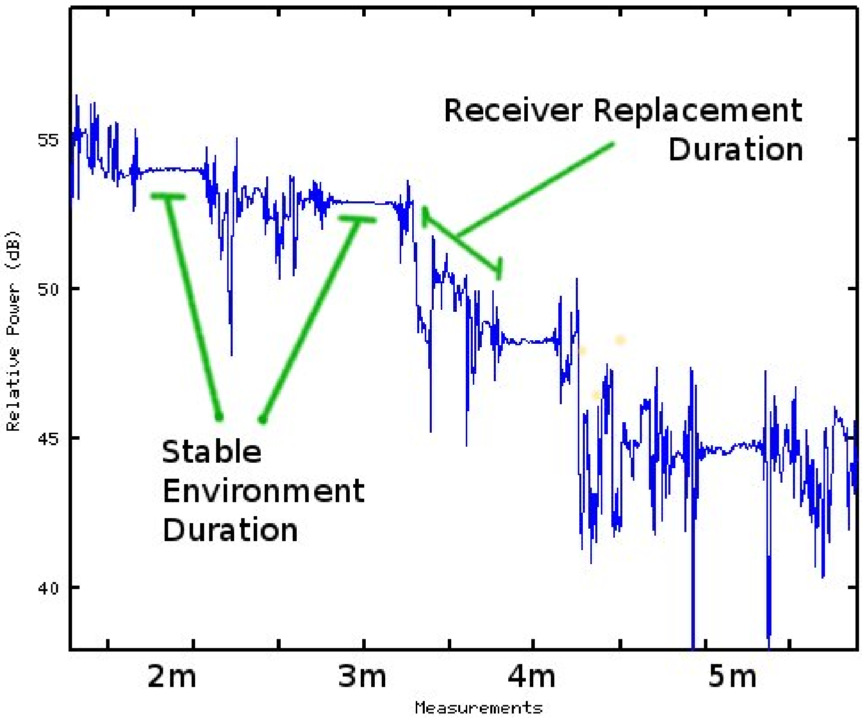

Figure 4.2. RSS values taken during the measurements where the distance between the transmitter and the receiver varies from 2m to 5m.

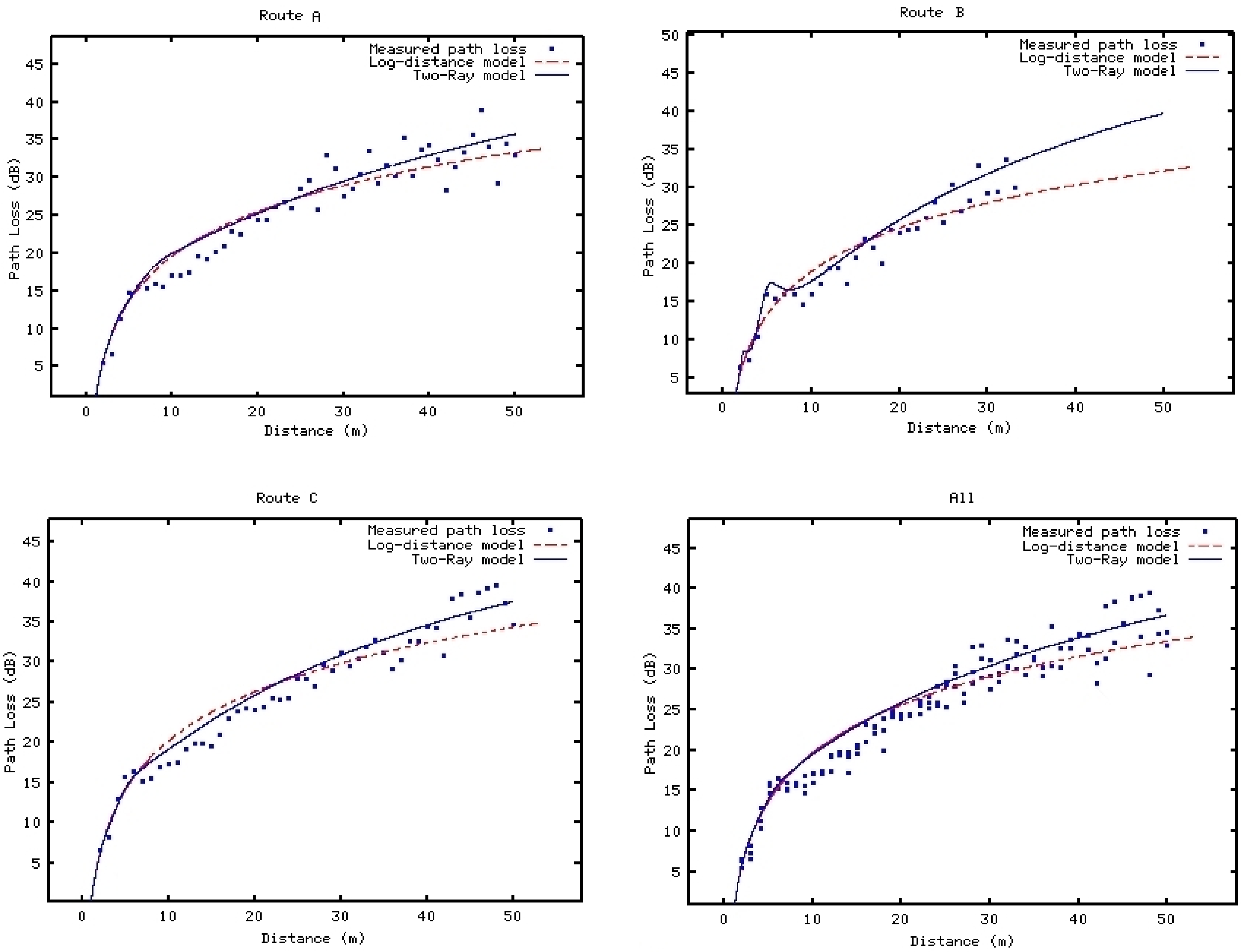

Figure 4.3. Measured path loss values for different routes and their fittings to models.

When the averages are calculated for the measurements from different distances, each pair of distance-RSS measurements are recorded. Then, the relative path-loss (dB) values are obtained by subtracting each RSS_i from the reference value (RSS_1). The reference value RSS_1 is the RSS value at 1 meter distance from the transmitter. Since we can't measure the transmitted power, we can't consider the path loss PL_i for each measurement, instead, we always consider the relative path loss $PL_i - PL_0$ which is equal to $RSS_1 - RSS_i$.

For the measured path loss data, we fit some of the most common path loss models used for short range LoS channels to determine the best fitting path loss model for our test area: two-ray ground reflection model and log-distance model. Figure 4.3(a,b,c) shows a plot of three different set of measurements taken for three different routes, with the same transmitter and receiver heights (H_t=1m and H_r=1m).

Table 4.1. Mean-square errors for three different set of measurements (1-50m).

Measurement	Two-Ray Error	Log-Distance Error
A	5.485	5.508
B	4.261	5.02
C	3.68	6.319
A+B+C	5.25	6.091

When the path loss values from these three different set of measurements are concatenated, the data plotted in the last graphic in Figure 4.3(All) is achieved, and the log-distance and two-ray models are also fitted using least-squares method to this data.

As seen from Figure 4.3, there is no significant fitness difference between the two models to represent the data from the measurements. Table 4.1 shows the calculated mean-square errors for all four cases shown in Figure 4.3 for both two-ray and log-distance models.

To comment on the Figure 4.3, because of the fitting behavior of the least squares estimation, the log-distance path loss curve usually overestimates the measurement data with distance between 5 and 20 meters, and it underestimates the data with longer distances after 25 meters. Since the estimation method always tends to minimize the square error, it tries to keep the curve close to all of the data. This behavior of the measured data shows that the path loss curve (determined by the path loss exponent γ) is changeable for the data collected for different intervals of distances.

When the distance gets longer, the effect of the environment and the ground shape increases. To determine the better path loss model for a shorter distance interval like 25m, the first 1-25m part of the same measurement sets are considered and path loss models are also fit to that short range data. Figure 4.4 shows the fitting path loss curves to the short-range (25m) part of the data shown in Figure 4.3. Table 4.2 shows the mean-square error values for the data in Figure 4.4. These results imply that the two-ray model fits slightly better to the path-loss data measured for the environment,

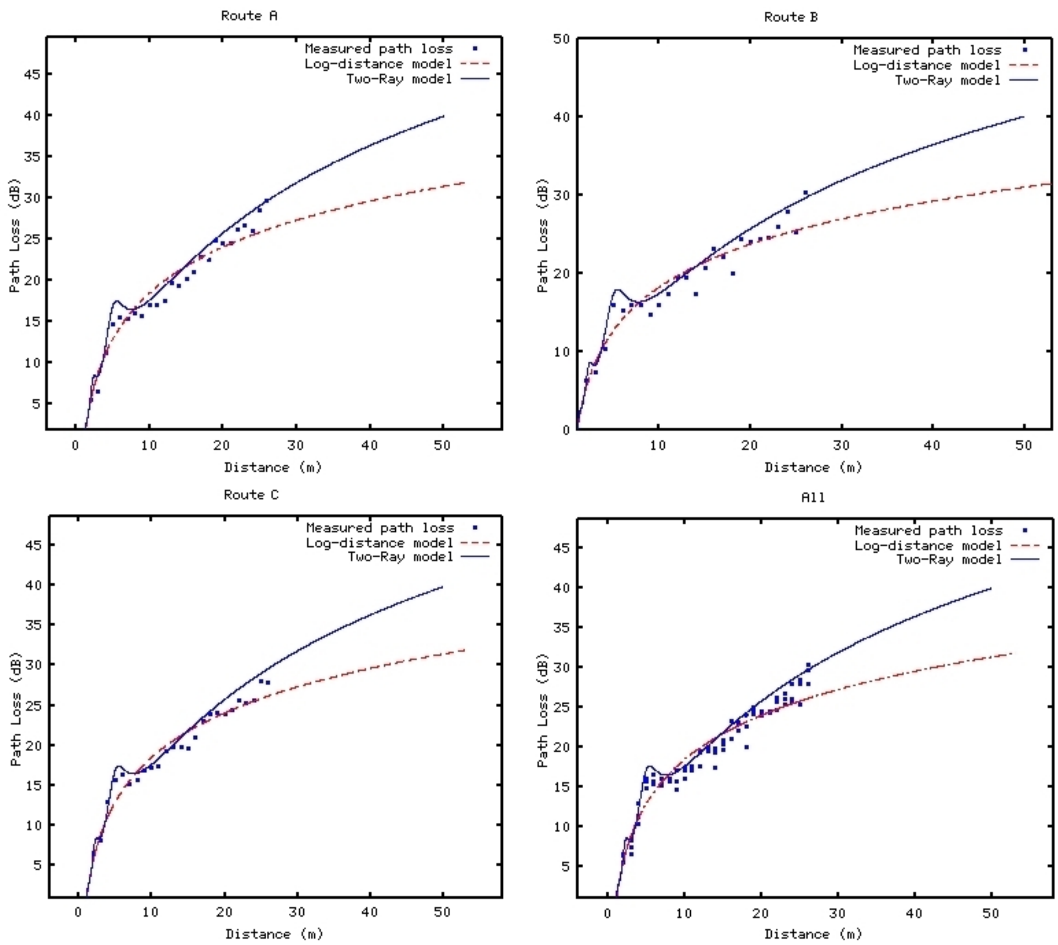

Figure 4.4. Fitting the models to 1-25 m samples of the same data.

Table 4.2. Mean-square errors for three different set of measurements (1-25m).

Measurement	Two-Ray Error	Log-Distance Error
A	1.938	2.458
B	3.525	3.489
C	1.806	1.639
A+B+C	2.430	2.554

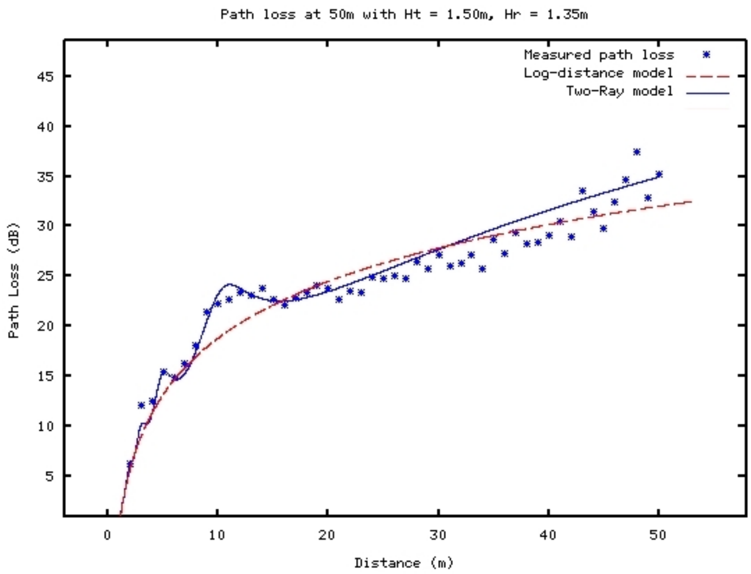

Figure 4.5. Fitting path-loss values with a higher transmitter-receiver pair.

but neither of these models are dominant over each other too much.

Comparing the results shown in the Figure 4.3 and the Figure 4.4, one may say that the behavior of the fitting curve of the two-ray model changes for the dataset of a shorter distance interval, and the two models becomes less like each other. The reason for this is the phase difference between the direct wave and the reflecting wave forming the calculated power in the two ray model becomes more dominant in shorter distances, and these two rays make a more remarkable constructive/destructive effect on each other. When the distance d between the transmitter and the receiver gets longer, the effect of the reflecting wave gets less significant and the curve becomes more like a logarithmically increasing function like the log distance model.

Another set of measurements is performed on the Route C with different transmitter and receiver heights: H_t=1.50m and H_r=1.35m (Figure 4.5). Fitting these data to two-ray ground reflection model also returns a much better mean square error (2.549) than the log-distance model (4.026). This result shows that the two-ray ground reflection model fits better to the data when the transmitter and receiver are higher.

Calculations also show that for shorter distance intervals like 1 to 25 meters, the two-ray model fits better to the measurement data. When the distance gets longer, H_t and H_r become small compared to d, and the effect of the reflected wave becomes less important.

As a result of these experiments, a system for measuring the RSS values over a field for different distances is built, and it is used to determine the most appropriate path-loss model for the environment. Since our field of experiments is short range and all the measurements are LoS, the two-ray ground reflection is found to be the most appropriate model.

4.2. Transmitter Location Estimation

For the measurements to perform transmitter location estimation, the field is filled with 20 wooden stands, each 1 meter high, to serve as holders for the receivers. These stands form a grid with 5 meter edges. Figure 4.6 shows the receiver locations at the top of the stands marked with red dots for illustration. The black grid lines are also drawn for the visualization of the placements.

To perform transmitter localization experiments, a series of measurements are done in the field using the stable receiver locations shown in Figure 4.6. The transmitter is placed on a stable tripod, and a set of measurements (100 power measurements in 25 seconds) are taken from each receiver location. This operation is repeated 5 times with different transmitter placements. Figure 4.7 shows the stable receiver locations and the transmitter placements. For each transmitter location (X_{T_i}, Y_{T_i}) and for each receiver location (X_{R_j}, Y_{R_j}), measurements RSS_{ij} are recorded. Transmitter and receiver heights are H_t=1.35m and H_r=1.35m for all measurements. Figure 4.8 shows

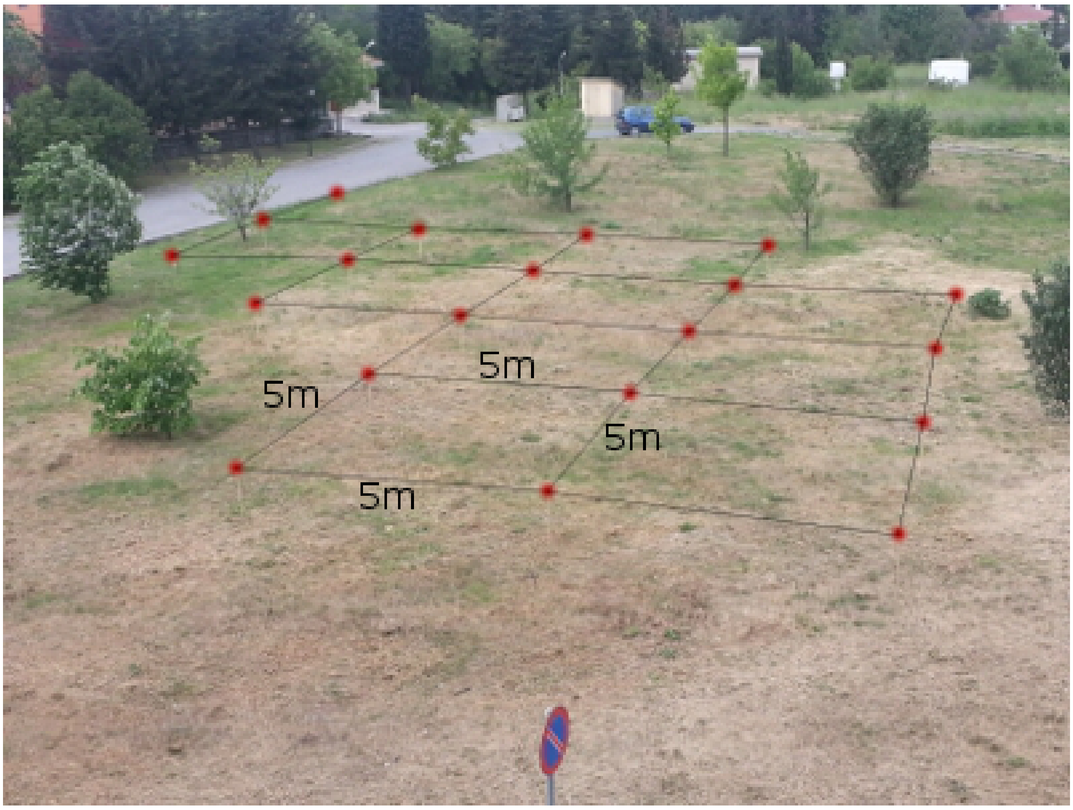

Figure 4.6. The field with wooden receiver stands.

the path loss values over distances for each set of these measurements with different transmitter locations.

To determine a better path loss function for the field with wooden stands, all the measured path loss values are gathered together and plotted against their known distances (Figure 4.9). Then, the two-ray and the log-distance path loss models are fit to the data. The result of this fitting shows that the two-ray model is much better than the log-distance model for this particular case of the field. The mean-square errors of the two-ray and the log-distance models are 6.5761 dB and 10.796 dB, respectively.

The path-loss data of these field measurements shown in Figure 4.9 are more dispersed than the data shown in Figure 4.3, because these field measurements are not taken along a single path. Instead, these measurements are taken at the transmitter and receiver positions shown in Figure 4.7. Furthermore the field has the wooden receiver stands forming a grid as an obstacle for the ground-reflecting wave, which has

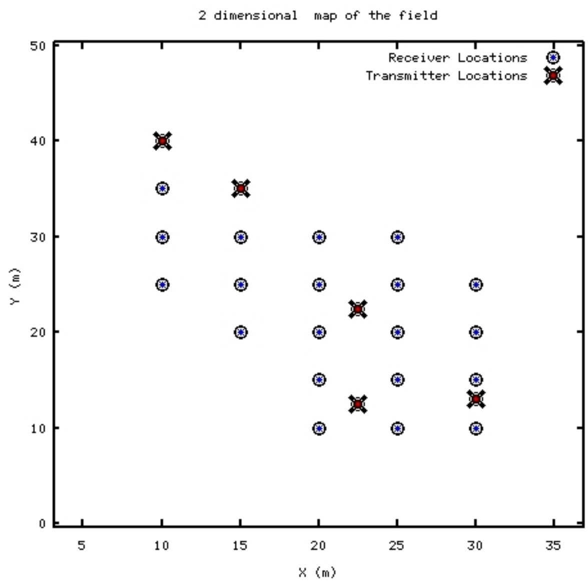

Figure 4.7. Two dimensional representation of the test field.

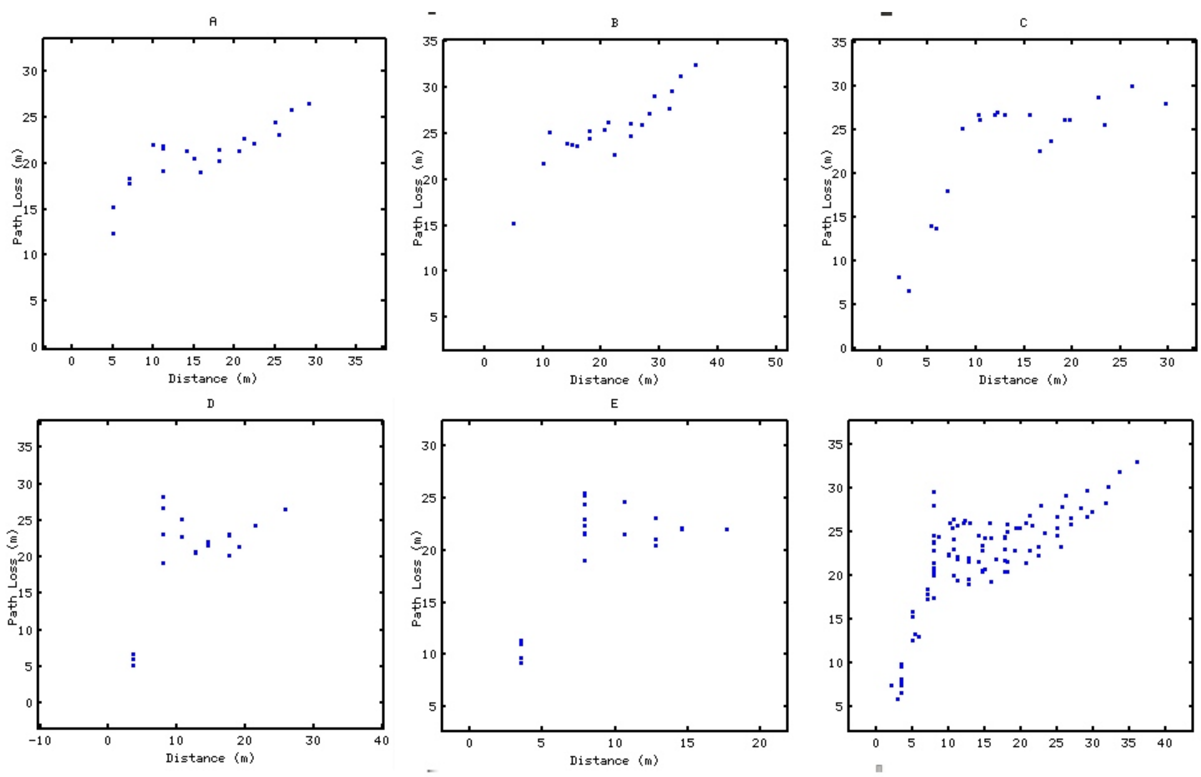

Figure 4.8. Distance - path loss values for each set of measurements with different transmitter location.

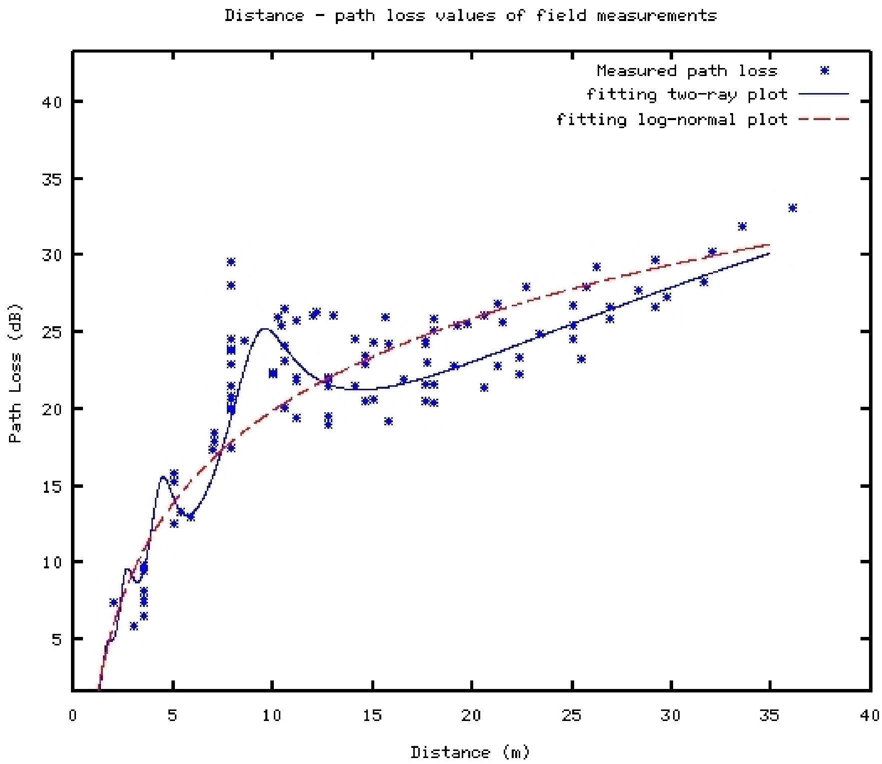

Figure 4.9. Distance - path loss values of all the measurements in the field.

significant importance on the RSS value. This situation is explained in more detail in Section 5.1 and Figure 5.2.

4.2.1. Estimation Using Two-Ray Model

To estimate the location of the stable transmitter, the RSS measurements from all or some of the 20 receivers are considered. To choose the most likely transmitter position, an exhaustive search is applied to the map with 0.5m intervals of x and y, and for each position, the square errors for each receiver are calculated by comparing the measured data and the model assuming the current search position is the transmitter location. The position with the least total square error is considered to be the selected transmitter location.

While estimating the most likely location using total least square error for each transmitter location, different number of receivers are considered. X receivers with the highest RSS values are taken into account for X is between 1 and 20. Figure 4.10

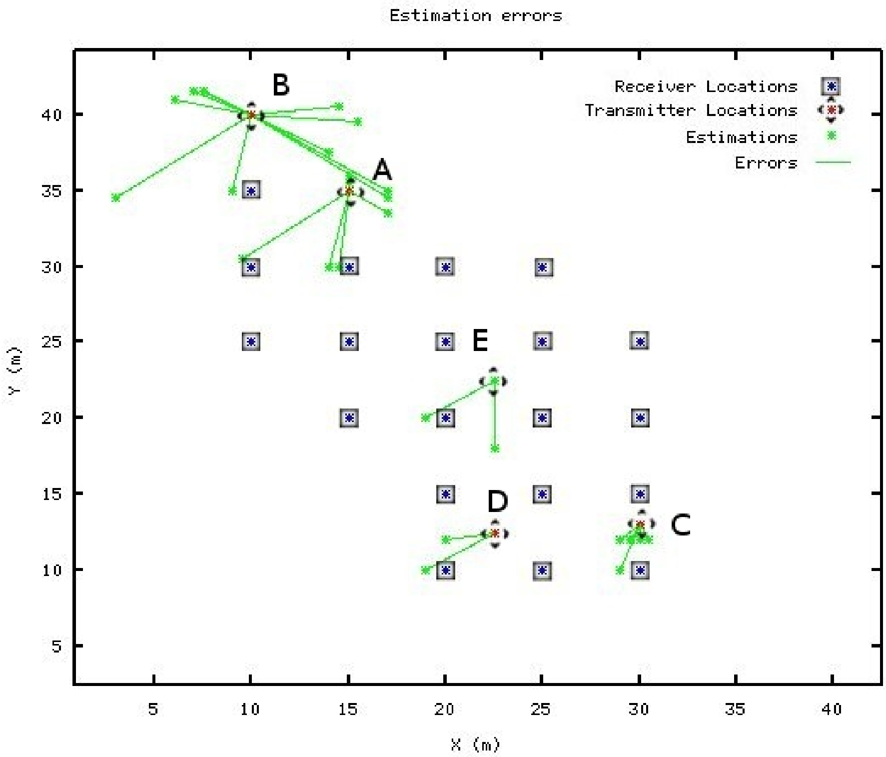

Figure 4.10. Location estimations for different sets of receivers using two-ray model.

shows each receiver and each estimation using different number of receivers for each transmitter, and errors of these estimations. Some of the estimations are overlapping.

The effect of taking X receivers with highest RSS value on the estimation error is shown in Figure 4.11. Its average graphic shows that taking higher count of receivers with the highest RSS value into calculation returns a better estimation. Taking the mean errors of five different cases (A,B,C,D,E) into account, the minimum average error is obtained with 13 receivers with highest RSS. Figure 4.12 shows the results of this estimation.

4.2.2. Estimation Using Log Distance Model

Following the same exhaustive search explained in Section 4.2.1, transmitter location is estimated by calculating the total square errors of each discrete point in the map using the log distance model. The point with the least total square error is selected as the transmitter location. Different sets of receivers with different receiver

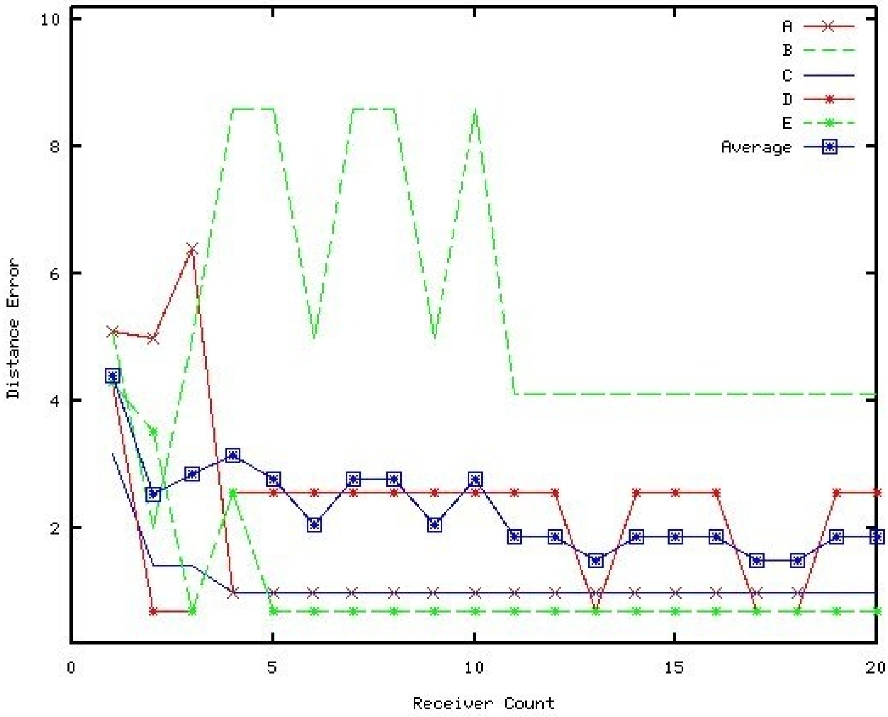

Figure 4.11. Location estimation errors for different receiver counts using two-ray model.

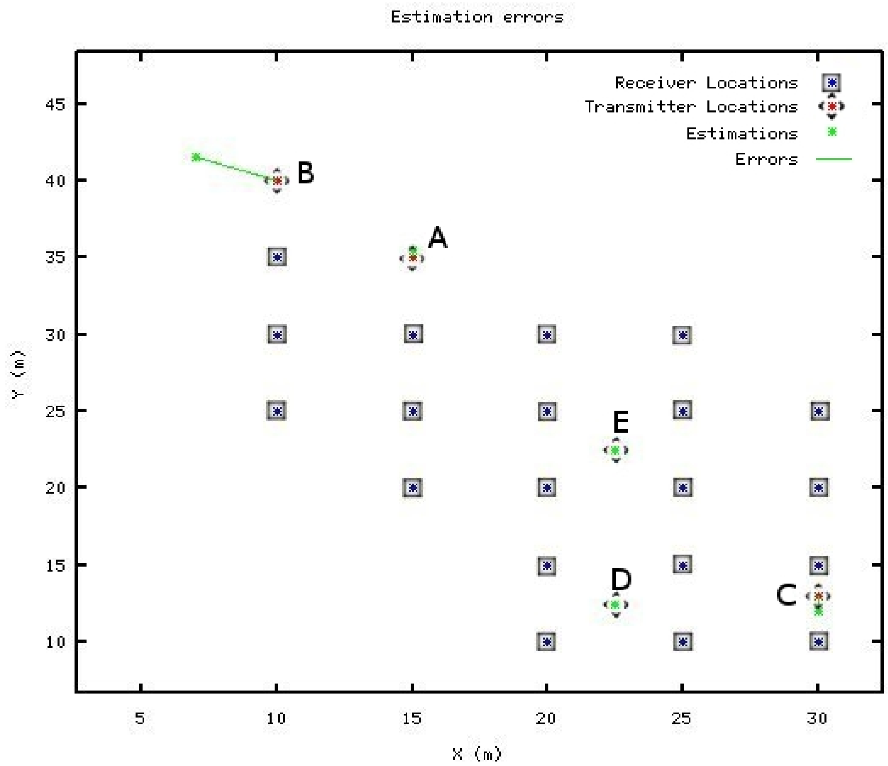

Figure 4.12. Location estimation errors for two-ray model using 13 receivers with highest RSS.

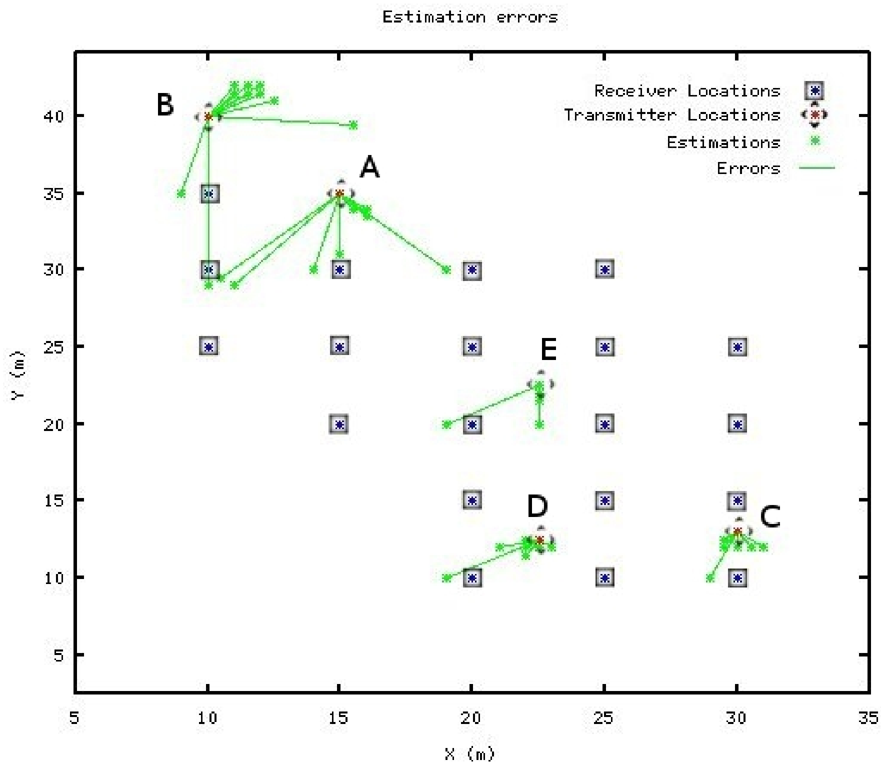

Figure 4.13. Location estimations for different sets of receivers using log distance model.

counts (1 to 20) are considered. Figure 4.13 shows different estimations with these sets. Some of the estimations are overlapping.

The effect of taking X receivers with highest RSS values on the estimation error is shown in Figure 4.14. Its average graphic shows that taking higher count of receivers with the highest RSS values into calculation returns a better estimation. Taking the mean errors of five different cases (A,B,C,D,E) into account, the minimum average error is obtained with 14 receivers with highest RSS. Figure 4.15 shows the results of this estimation.

4.2.3. Estimation Using LIvE REM Construction Technique with Log-Distance Model

To estimate the location of the stable transmitter, the location estimation method from the LIvE REM construction technique [2] is used. This technique makes use of

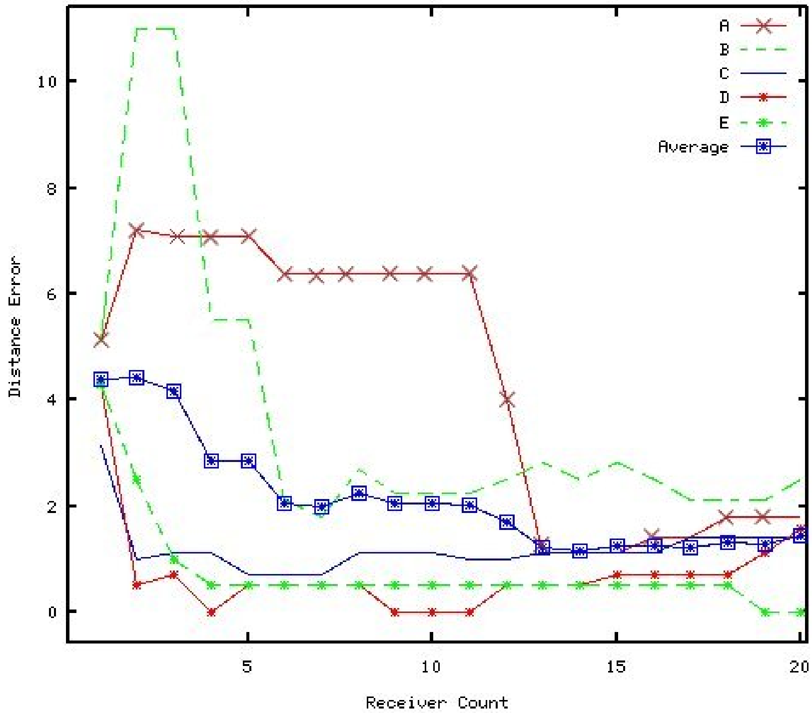

Figure 4.14. Location estimation errors for different receiver counts using log distance model.

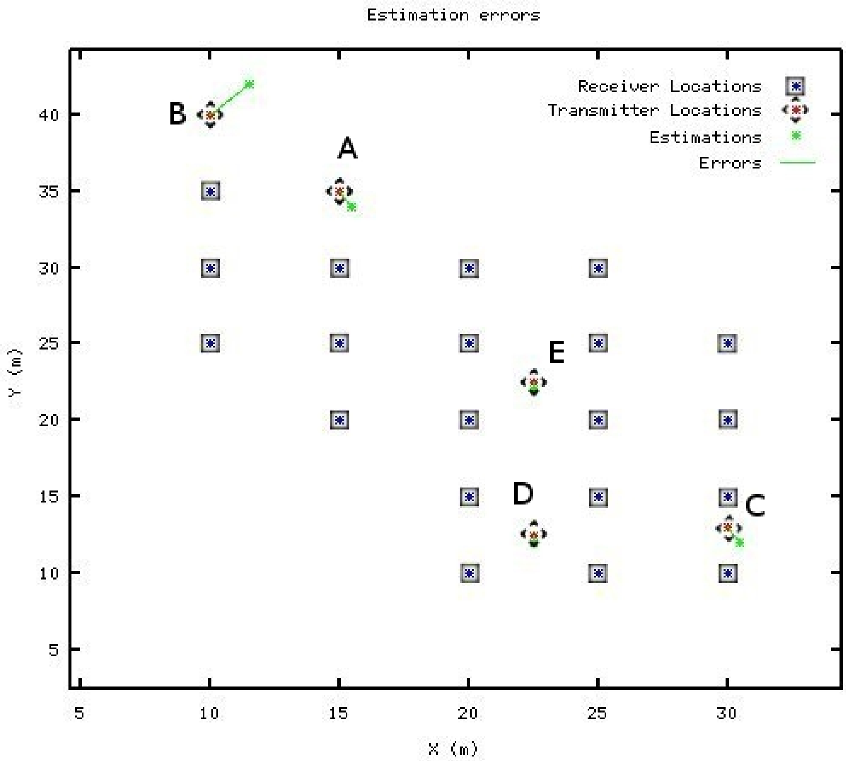

Figure 4.15. Location estimation errors for log distance model using 14 receivers with highest RSS.

the simplicity of the log distance model and formulates the problem to a matrix form.

If there is no disturbance in the measurements in [dB], then

$$10\gamma \log_{10}(d_{x_i,y_i}) \approx P_{tx} - PL_0 - \overline{P_{rx_i}} \tag{4.1}$$

where γ is the path loss exponent, d_{x_i,y_i} is the distance (m) of the i_{th} receiver to the transmitter, P_{tx} is the transmission power, PL_0 is the path loss in 1 meter, and $\overline{P_{rx_i}}$ is the RSS value of i_{th} receiver. Hence,

$$\sqrt{(x_t - x_i)^2 + (y_t - y_i)^2} \approx 10^{\frac{P_{tx} - PL_0 - \overline{P_{rx_i}}}{10\gamma}}. \tag{4.2}$$

Therefore,

$$(x_t - x_i)^2 + (y_t - y_i)^2 \approx 10^{\frac{P_{tx} - PL_0 - \overline{P_{rx_i}}}{5\gamma}} \tag{4.3}$$

where x_t,y_t is the transmitter location and x_i,y_i is the location of the i_{th} receiver. Consequently,

$$(x_t^2 - 2x_t x_i + x_i^2) + (y_t^2 - 2y_t y_i + y_i^2) \approx 10^{\frac{P_{tx} - PL_0 - \overline{P_{rx_i}}}{5\gamma}} \tag{4.4}$$

which results in

$$x_i^2 + y_i^2 \approx 2x_t x_i + 2y_t y_i + 10^{\frac{P_{tx} - PL_0 - \overline{P_{rx_i}}}{5\gamma}} - R^2 \tag{4.5}$$

where $R^2 = x_t^2 + y_t^2$. Then, we can express this equation in the matrix form $A\Theta \approx b$ where

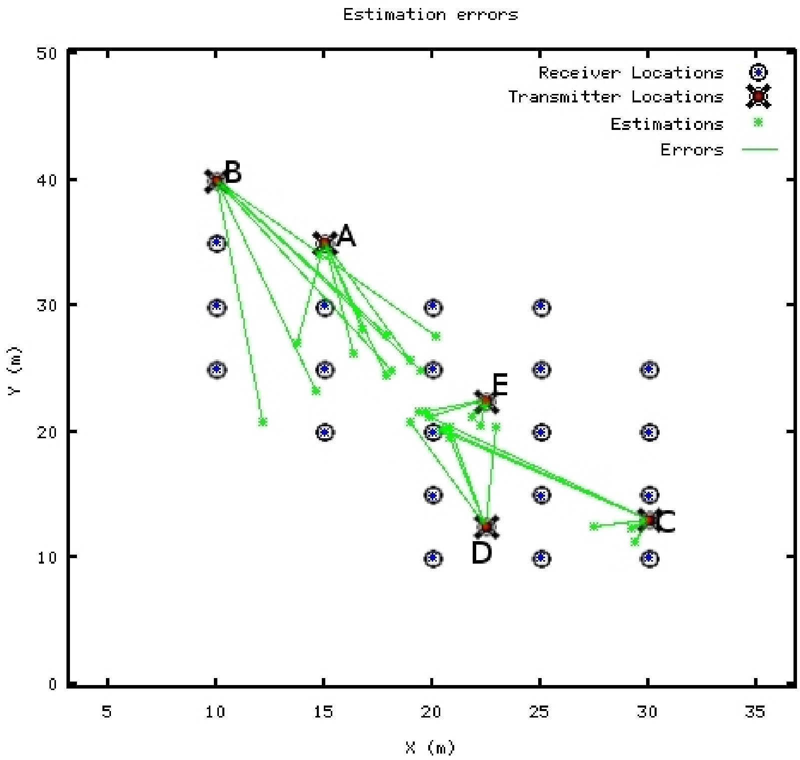

Figure 4.16. Location estimations with LIvE REM construction method using different count of receivers are with highest RSS.

$$A = \begin{pmatrix} 2x_1 & 2y_1 & 10^{\frac{-\overline{Prx_1}}{5\gamma}} & -1 \\ 2x_2 & 2y_2 & 10^{\frac{-\overline{Prx_2}}{5\gamma}} & -1 \\ . & . & . & . \\ . & . & . & . \\ 2x_n & 2y_n & 10^{\frac{-\overline{Prx_n}}{5\gamma}} & -1 \end{pmatrix}, \Theta = \begin{pmatrix} x_t \\ y_t \\ 10^{\frac{P_{tx}-PL_0}{5\gamma}} \\ R^2 \end{pmatrix}, b = \begin{pmatrix} x_1^2 + y_1^2 \\ x_2^2 + y_2^2 \\ . \\ . \\ x_i^2 + y_i^2 \end{pmatrix}.$$

Let $\widehat{\Theta}$ be the estimated value for Θ. Then, the solution is computed as

$$\widehat{\Theta} = (A^T A)^{-1} A^T b \tag{4.6}$$

The method requires at least 4 different receiver measurements. For that reason, different count of receivers are considered. X receivers with the highest RSS value are taken into account for X = [4,5,7,10,14,20].

Figure 4.16 shows each receiver and each estimation using different count of

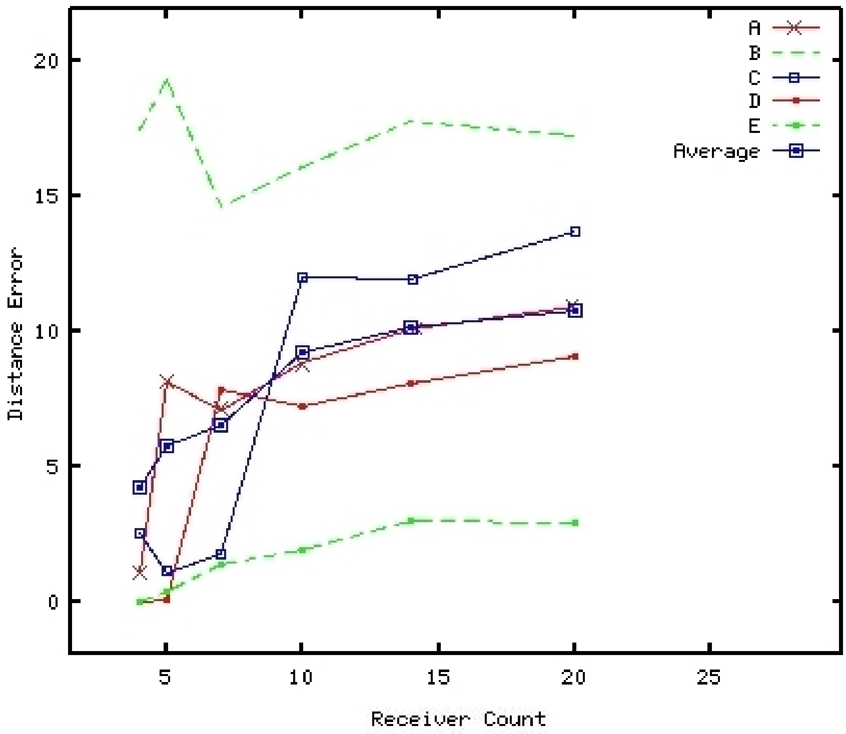

Figure 4.17. Location estimation errors for different receiver counts using LIvE REM.

receivers for each transmitter, and errors of these estimations. Some of the estimations are overlapping.

The effect of taking X receivers with highest RSS value to the estimation error is shown in Figure 4.17. Its average graphic shows that taking four receivers with the highest RSS value into calculation returns the best estimation. For this case with log-distance model, transmitter location is estimated using only four highest RSS value. Figure 4.18 shows the results of this estimation.

By looking at the results the Figure 4.18, one can claim that the LIvE REM construction method returns much better results when the transmitter is equally surrounded by receivers. It can even estimate the exact location of the transmitter for cases E and D, where the transmitter is actually between four receivers. For cases A and C, it also estimates a pretty close location where the transmitter is partially surrounded by receivers. For the case B, where the transmitter is out of the receiver area, the estimation tends to bias into the place where the receivers are more dense.

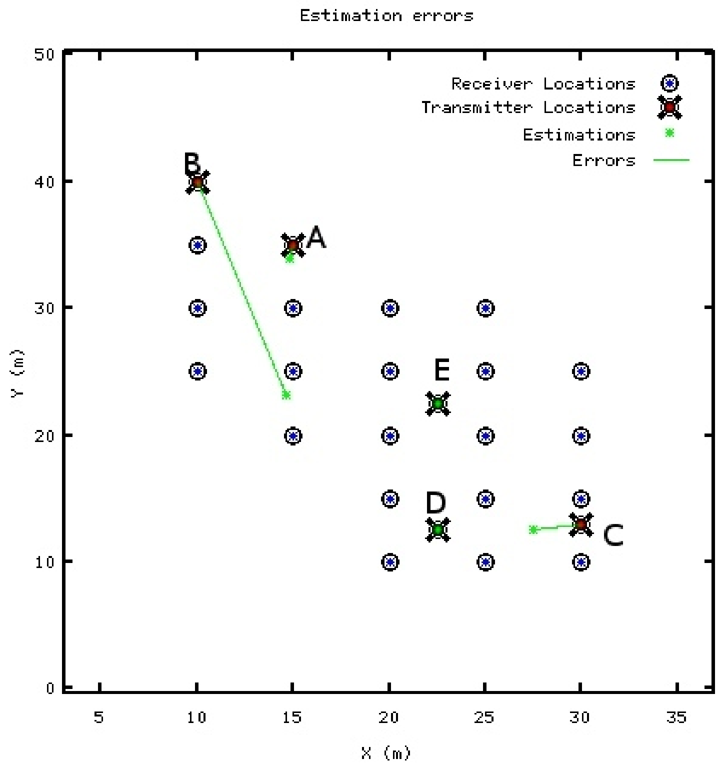

Figure 4.18. Location estimation errors for LIvE REM construction method with 4 receivers with highest RSS.

These results show that the LIvE REM construction method's estimation is almost as accurate as the exhaustive search methods with least squares estimation when four receivers with highest RSS are taken into account. However, it doesn't utilize the information from the receivers which are relatively far, as much as the least squares methods do. Figure 4.19 shows the comparison of the mentioned three estimation's average estimation errors for transmitters with five different locations. As the considered receiver count increases, the estimation of LIvE REM gets worse.

The applicability of the LIvE REM method's estimation comes from its low complexity [2]. Since the exhaustive search methods mentioned in Section 4.2.1 and 4.2.2 have complexity growing exponentially with the map resolution and the sensor count, they are much slower. However, they are applied and explained to exploit the maximum possible information usage from the RSS values.

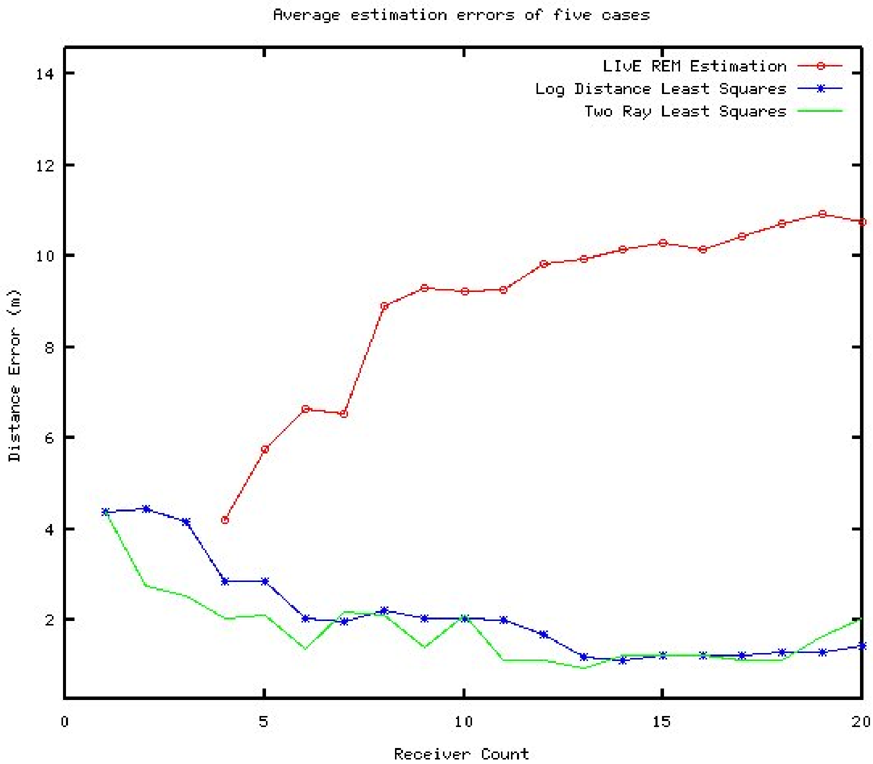

Figure 4.19. Comparison of average location estimation errors for three different methods.

5. CONCLUSIONS

5.1. Practical Experiences

Since this is a practical implementation and a measurement based work rather than a theoretical one, we encountered a lot of technical challenges, physical problems and operational difficulties. While dealing with them, we earned serious practical experience, which might be useful for people who plan to conduct similar experiments. These experiences are explained in this section.

To begin with, using a lower-level signal processing software provides a significant performance boost. At the beginning of this project, we used GNURadio open source signal processing software toolkit to read raw samples from RTL-SDR and process them to make power calculations. However, it turned out that the software was using much higher percentage of the CPU than it should do. The reason of this situation was the modular structure of the GNURadio, in which each block has its own thread and looping program, to perform a signal stream from source to sink.

Instead of using toolkits like GNURadio or Labview, we developed our own C++ program, which uses RTL-SDR's own driver library to get the raw samples from the device, and uses Linux built-in FFT library to get the power spectrum directly from the raw samples. Since the only function of the program is calculating the received signal power, such software components were enough rather than using a whole Digital Signal Processing toolkit. Writing such a program made the process much faster and easier to manage.

All of the RTL-SDR dongles have a center frequency error, which can be measured and corrected at runtime or manually by applying a calibration factor. It is caused by the imperfection of the local oscillator, and the amount of the error is affected mainly by the ambient temperature. Since a single receiver is used for all measurements in this work, its frequency error is measured as approximately 35 KHz and the correction factor is applied. The changes in the error caused by the temperature changes were insignificant for calculation of the RSS measurements.

Experiments showed that battery condition of the transmitter can change the power of the transmission. Thus, the RSS values are also affected by the battery condition. Keeping the transmission power stable is important for quality of the results. For this reason, the transmitter is powered with an external power adapter shown in Figure 3.1, which is connected to one of the university building's power plugs via a power extension cable.

The antenna shape and size is crucial for the RSS value of a measurement. While using the typical RTL-SDR receiver, results of the measurements with different antenna-cable placements showed that the shape and the position of the antenna cable makes a significant difference on the RSS value. This proved that the antenna cable also receives significant amount of signal. Figure 5.1 shows the antenna and an arbitrary placement of its cable. To minimize the effect of the antenna cable's placement, the antenna configuration explained in Section 3.2.2.2 is applied, which is shown in detail in Figure 3.4.

Transmitter and receiver antenna heights completely change the path loss character of a LoS channel, because the wave reflecting from the ground has a significant effect on the RSS value. Before starting an experiment, it is important to consider possible sources of interruption (obstacles) and the reflection. The most significant reflection source is the ground for a LoS open field transmission.

Our path loss measurements shown in this work (Section 4.1) has a better fit, and more stable distribution compared to the field measurements done for location estimation (Section 4.2). The reason for this is there might be other wooden receiver stands between the transmitter and the receiver. These stands do not interrupt the line of sight wave from transmitter to receiver because they both have their own elevation, but when they are on the path, they interrupt the ground-reflecting wave. Figure 5.2 shows a typical case for this situation.

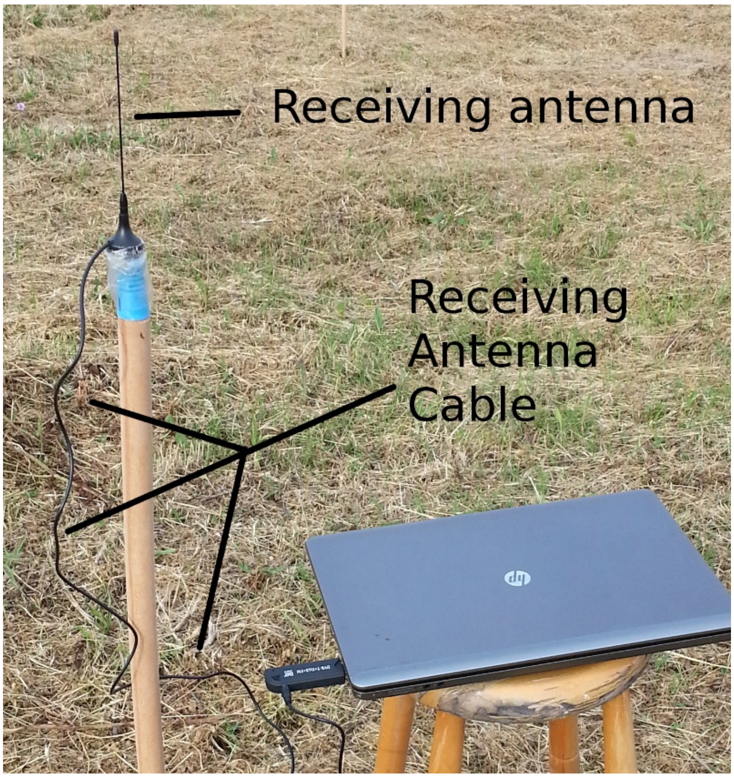

Figure 5.1. An unstable and unpredictable antenna configuration for RTL-SDR receiver.

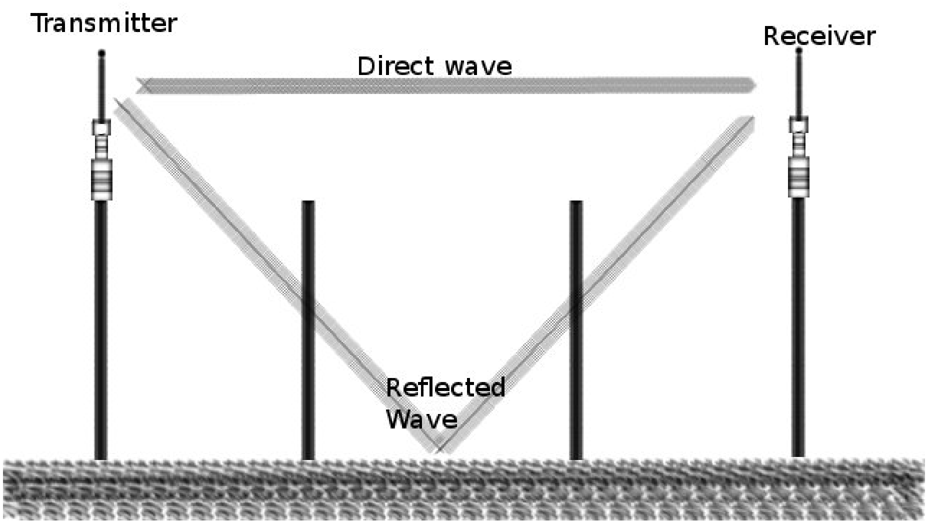

Figure 5.2. A typical case of our field measurements.

Calculations also show that when the location of a transmitter is being estimated, while using same count of receivers, using the ones with higher RSS (meaning the closer ones) returns much better result compared to using the ones with lower RSS. This result implies that deploying the receivers with shorter intervals and considering the RSS data of the closer receivers with a higher weight improves the estimation quality.

5.2. Summary

The work in this thesis can be summarized as follows:

- Cognitive Radio, Dynamic Spectrum Access, Spectrum Sensing and Radio Environment Map concepts are explained.
- A testbed is created using SDR devices to perform spectrum sensing experiments. With the data from those experiments, path loss character of an open field is examined.
- Feasibility of implementing transmitter location estimation in an open field with SDR is examined. A method is proposed to estimate the transmitter location using the received data. Another given method named LIvE REM Construction [2] is also applied to the measured data and the estimation results of these two methods are compared.
- Practical issues and technical difficulties of setting up a testbed in an open field for transmitter location estimation using SDR devices are discussed.

5.3. Future Work

As a future work in cooperative sensing, we plan to apply the transmitter location estimation methods mentioned in this thesis to estimate the location of mobile transmitters since the CR users are more likely to be mobile devices. To achieve this goal, other decision techniques might also be introduced into the system like Kalman filters.

The receivers in this work listen to the same band since the transmitter used in this system has a fixed transmission frequency. However, the receivers can be tuned to listen to different bands since they are SDRs. Since a REM is a multi-domain information system, we plan to improve this system so that it can listen to different bands periodically.

To construct a REM in a large real-world area, it is essential to know the propagation model of the environment. Thus, we also plan to take measurements for further distances to determine appropriate path loss models and their parameters for non-LoS channels.

The ultimate goal of designing the testbed and making transmitter location estimation experiments in this work is to construct a REM. To keep the data in a systematic way, we plan to create a REM database architecture and a cognitive engine as a central decision unit. Automating the RSS feed, we plan to work on the spectrum decision mechanism.

REFERENCES

1. Sun, H., A. Nallanathan, C.-X. Wang, and Y. Chen, “Wideband Spectrum Sensing for Cognitive Radio Networks: A survey”, *Wireless Communications, IEEE*, Vol. 20, No. 2, pp. 74–81, 2013.

2. Yılmaz, H. B., *Cooperative Spectrum Sensing and Radio Environment Map Construction in Cognitive Radio Networks*, Ph.D. thesis, Bogaziçi University, 2012.

3. Akl, R. G., D. Tummala, and X. Li, “Indoor Propagation Modeling at 2.4 GHz for IEEE 802.11 Networks”, 2006.

4. Mitola, J. and G. Q. Maguire Jr, “Cognitive Radio: Making Software Radios More Personal”, *Personal Communications, IEEE*, Vol. 6, No. 4, pp. 13–18, 1999.

5. Haykin, S., “Cognitive Radio: Brain-Empowered Wireless Communications”, *Selected Areas in Communications, IEEE Journal on*, Vol. 23, No. 2, pp. 201–220, 2005.

6. Cabric, D., S. M. Mishra, and R. W. Brodersen, “Implementation Issues in Spectrum Sensing for Cognitive Radios”, *Signals, systems and computers, 2004. Conference record of the thirty-eighth Asilomar conference on*, Vol. 1, pp. 772–776, IEEE, 2004.

7. Yilmaz, H. B., T. Tugcu, and S. Bayhan, “Radio Environment Map as Enabler for Practical Cognitive Radio Networks”, *Communications Magazine, IEEE*, Vol. 51, No. 12, pp. 162–169, 2013.

8. Akyildiz, I. F., W.-Y. Lee, M. C. Vuran, and S. Mohanty, “NeXt Generation/Dynamic Spectrum Access/Cognitive Radio Wireless Networks: A Survey”, *Computer Networks*, Vol. 50, No. 13, pp. 2127–2159, 2006.

9. Jondral, F. K., “Software-Defined Radio: Basics and Evolution to Cognitive Radio”, *EURASIP journal on wireless communications and networking*, Vol. 2005, No. 3, pp. 275–283, 2005.

10. Wild, B. and K. Ramchandran, “Detecting Primary Receivers for Cognitive Radio Applications”, *New Frontiers in Dynamic Spectrum Access Networks, 2005. DySPAN 2005. 2005 First IEEE International Symposium on*, pp. 124–130, IEEE, 2005.

11. Wang, B. and K. R. Liu, “Advances in Cognitive Radio Networks: A Survey”, *Selected Topics in Signal Processing, IEEE Journal of*, Vol. 5, No. 1, pp. 5–23, 2011.

12. Kolodzy, P. J., “Interference Temperature: A Metric for Dynamic Spectrum Utilization”, *International Journal of Network Management*, Vol. 16, No. 2, pp. 103–113, 2006.

13. Lu, Q., W. Wang, W. Wang, and T. Peng, “Asynchronous Distributed Power Control under Interference Temperature Constraints”, *Global Telecommunications Conference, 2008. IEEE GLOBECOM 2008. IEEE*, pp. 1–5, IEEE, 2008.

14. Ghasemi, A. and E. S. Sousa, “Collaborative Spectrum Sensing for Opportunistic Access in Fading Environments”, *New Frontiers in Dynamic Spectrum Access Networks, 2005. DySPAN 2005. 2005 First IEEE International Symposium on*, pp. 131–136, IEEE, 2005.

15. Gardner, W. A., “Signal Interception: A Unifying Theoretical Framework for Feature Detection”, *Communications, IEEE Transactions on*, Vol. 36, No. 8, pp. 897–906, 1988.

16. Hoven, N., R. Tandra, and A. Sahai, “Some Fundamental Limits on Cognitive Radio”, *Wireless Foundations EECS, Univ. of California, Berkeley*, 2005.

17. Digham, F. F., M.-S. Alouini, and M. K. Simon, "On the Energy Detection of Unknown Signals over Fading Channels", *IEEE Transactions on Communications*, Vol. 55, No. 1, pp. 21–24, 2007.

18. Eryigit, S. and T. Tugcu, "Joint Channel and User Selection for Transmission and Sensing in Cognitive Radio Networks", *Cognitive Radio Oriented Wireless Networks and Communications (CROWNCOM), 2012 7th International ICST Conference on*, pp. 54–59, IEEE, 2012.

19. Eryigit, S., S. Bayhan, and T. Tugcu, "Energy-Efficient Multichannel Cooperative Sensing Scheduling with Heterogeneous Channel Conditions for Cognitive Radio Networks", *Vehicular Technology, IEEE Transactions on*, Vol. 62, No. 6, pp. 2690–2699, 2013.

20. Yilmaz, H. B. and T. Tugcu, "Location Estimation-Based Radio Environment Map Construction in Fading Channels", *Wireless Communications and Mobile Computing*, 2013.

21. Zhao, Y., B. Le, and J. H. Reed, "Network Support–The Radio Environment Map", *Cognitive radio technology*, pp. 325–366, 2006.

22. Subramani, S., J. Riihijarvi, B. Sayrac, L. Gavrilovska, M. Sooriyabandara, T. Farnham, and P. Mahonen, "Towards Practical REM-Based Radio Resource Management", *Future Network & Mobile Summit (FutureNetw), 2011*, pp. 1–8, IEEE, 2011.

23. Riihijarvi, J., P. Mahonen, M. Petrova, and V. Kolar, "Enhancing Cognitive Radios with Spatial Statistics: From Radio Environment Maps to Topology Engine", *Cognitive Radio Oriented Wireless Networks and Communications, 2009. CROWNCOM'09. 4th International Conference on*, pp. 1–6, IEEE, 2009.

24. Bolea, L., J. Pérez-Romero, R. Agustí, and O. Sallent, "Context Discovery Mechanisms for Cognitive Radio", *Vehicular Technology Conference (VTC Spring), 2011*

IEEE 73rd, pp. 1–5, IEEE, 2011.

25. Riihijarvi, J., J. Nasreddine, and P. Mahonen, "Demonstrating Radio Environment Map Construction from Massive Data Sets", *Dynamic Spectrum Access Networks (DYSPAN), 2012 IEEE International Symposium on*, pp. 266–267, IEEE, 2012.

26. Atanasovski, V., J. van de Beek, A. Dejonghe, D. Denkovski, L. Gavrilovska, S. Grimoud, P. Mahonen, M. Pavloski, V. Rakovic, and J. Riihijarvi, "Constructing Radio Environment Maps with Heterogeneous Spectrum Sensors", *New Frontiers in Dynamic Spectrum Access Networks (DySPAN), 2011 IEEE Symposium on*, pp. 660–661, IEEE, 2011.

27. Gezici, S., "A Survey on Wireless Position Estimation", *Wireless Personal Communications*, Vol. 44, No. 3, pp. 263–282, 2008.

28. Gustafsson, F. and F. Gunnarsson, "Mobile Positioning Using Wireless Networks: Possibilities and Fundamental Limitations based on Available Wireless Network Measurements", *Signal Processing Magazine, IEEE*, Vol. 22, No. 4, pp. 41–53, 2005.

29. Heusdens, R. and N. Gaubitch, "Time-Delay Estimation for TOA-Based Localization of Multiple Sensors", *Acoustics, Speech and Signal Processing (ICASSP), 2014 IEEE International Conference on*, pp. 609–613, IEEE, 2014.

30. Shao, H.-J., X.-P. Zhang, and Z. Wang, "Efficient Closed-Form Algorithms for AOA Based Self-Localization of Sensor Nodes Using Auxiliary Variables", *Signal Processing, IEEE Transactions on*, Vol. 62, No. 10, pp. 2580–2594, 2014.

31. Kvaksrud, T.-I., "Range Measurements in an Open Field Environment", *Texas Instrum. Incorporated, Dallas, TX, Design Note DN018*, 2008.

32. Abhayawardhana, V., I. Wassell, D. Crosby, M. Sellars, and M. Brown, "Comparison of Empirical Propagation Path Loss Models for Fixed Wireless Access

Systems", *Vehicular Technology Conference, 2005. VTC 2005-Spring. 2005 IEEE 61st*, Vol. 1, pp. 73–77, IEEE, 2005.

33. Sharma, P. K. and R. Singh, "Comparative Analysis of Propagation Path Loss Models with Field Measured Data", *International Journal of Engineering Science and Technology*, Vol. 2, No. 6, pp. 2008–2013, 2010.

34. Medeisis, A. and A. Kajackas, "On the Use of the Universal Okumura-Hata Propagation Prediction Model in Rural Areas", *Vehicular Technology Conference Proceedings, 2000. VTC 2000-Spring Tokyo. 2000 IEEE 51st*, Vol. 3, pp. 1815–1818, IEEE, 2000.